

Article

Provenance Response to Rifting and Separation at the Jan Mayen Microcontinent Margin

Andrew Morton ^{1,2,*}, David W. Jolley ², Adam G. Szulc ¹, Andrew G. Whitham ^{1,†}, Dominic P. Strogen ^{1,3}, C. Mark Fanning ⁴ and Sidney R. Hemming ⁵

¹ CASP, West Building, Madingley Rise, Cambridge CB3 0UD, UK

² Department of Geology and Geophysics, Meston Building, University of Aberdeen, Aberdeen AB24 3UE, UK

³ GNS Science, Lower Hutt 5040, New Zealand

⁴ Research School of Earth Sciences, Australian National University, Canberra, ACT 0200, Australia

⁵ Lamont Doherty Earth Observatory, Columbia University, Palisades, NY 10964, USA

* Correspondence: heavyminerals@hotmail.co.uk

† Deceased.

Abstract: The Eocene-Miocene successions recovered at DSDP sites on the Jan Mayen Ridge (NE Atlantic) and on the adjacent East Greenland margin provide a sedimentary record of the rifting and separation of the Jan Mayen Microcontinent from East Greenland. A combination of palynology, conventional heavy mineral analysis, single-grain major and trace element geochemistry and radiometric dating of amphibole and zircon has revealed a major change in sediment provenance took place at the Early/Late Oligocene boundary corresponding to a prominent seismic reflector termed JA. During the Eocene and Early Oligocene, lateral variations in provenance character indicate multiple, small-scale transport systems. Site 349 and Kap Brewster were predominantly supplied from magmatic sources (Kap Brewster having a stronger subalkaline signature compared with Site 349), whereas Site 346 received almost exclusively metasedimentary detritus. By contrast, Late Oligocene provenance characteristics are closely comparable at the two Jan Mayen sites, the most distinctive feature being the abundance of reworked Carboniferous, Jurassic, Cretaceous and Eocene palynomorphs. The Site 349 succession documents an evolution in the nature of the magmatic provenance component. Supply from evolved alkaline magmatic rocks, such as syenites, was important in the Middle Eocene and lower part of the Early Oligocene, but was superseded in the later Early Oligocene by mafic magmatic sources. In the latest Early Oligocene, the presence of evolved clinopyroxenes provides evidence for prolonged magmatic fractionation. Initial low degrees of partial melting led to generation of alkaline (syenitic) magmas. The extent of partial melting increased during the Early Oligocene, generating basaltic rocks with both subalkaline and alkaline compositions. Towards the end of the Early Oligocene, the amount of partial melting and magma supply rates decreased. In the Late Oligocene, there is no evidence for contemporaneous igneous activity, with scarce magmatic indicator minerals. The provenance change suggests that the hiatus at the Early/Late Oligocene boundary represents the initiation of the proto-Kolbeinsey Ridge and separation of the Jan Mayen Microcontinent from East Greenland.

Keywords: East Greenland; Jan Mayen; North Atlantic; rifting; provenance; Eocene; Oligocene



Citation: Morton, A.; Jolley, D.W.; Szulc, A.G.; Whitham, A.G.; Strogen, D.P.; Fanning, C.M.; Hemming, S.R. Provenance Response to Rifting and Separation at the Jan Mayen Microcontinent Margin. *Geosciences* **2022**, *12*, 326. <https://doi.org/10.3390/geosciences12090326>

Academic Editors: Ian Coulson and Jesus Martinez-Frias

Received: 18 July 2022

Accepted: 23 August 2022

Published: 29 August 2022

Publisher's Note: MDPI stays neutral with regard to jurisdictional claims in published maps and institutional affiliations.



Copyright: © 2022 by the authors. Licensee MDPI, Basel, Switzerland. This article is an open access article distributed under the terms and conditions of the Creative Commons Attribution (CC BY) license (<https://creativecommons.org/licenses/by/4.0/>).

1. Introduction and Geological Setting

The Jan Mayen Microcontinent (JMMC) is a fragment of continental crust that forms the submerged Jan Mayen Ridge, located mid-way between Norway and East Greenland (Figure 1). The JMMC is 400–450 km long and varies in width from 100 km in the north to 310 km in the south [1]. The continental nature of the JMMC crust is inferred on the basis of seismic refraction data [2–5], and has recently been proven by recovery of pre-breakup lithologies of Cretaceous, Jurassic and Permian-Triassic ages by gravity coring and dredging

along a steep escarpment on the southern Jan Mayen Ridge [6]. However, according to Kodaira et al. [2] and Brandsdóttir et al. [7], the crustal affinity of the southernmost area near Iceland remains less certain.

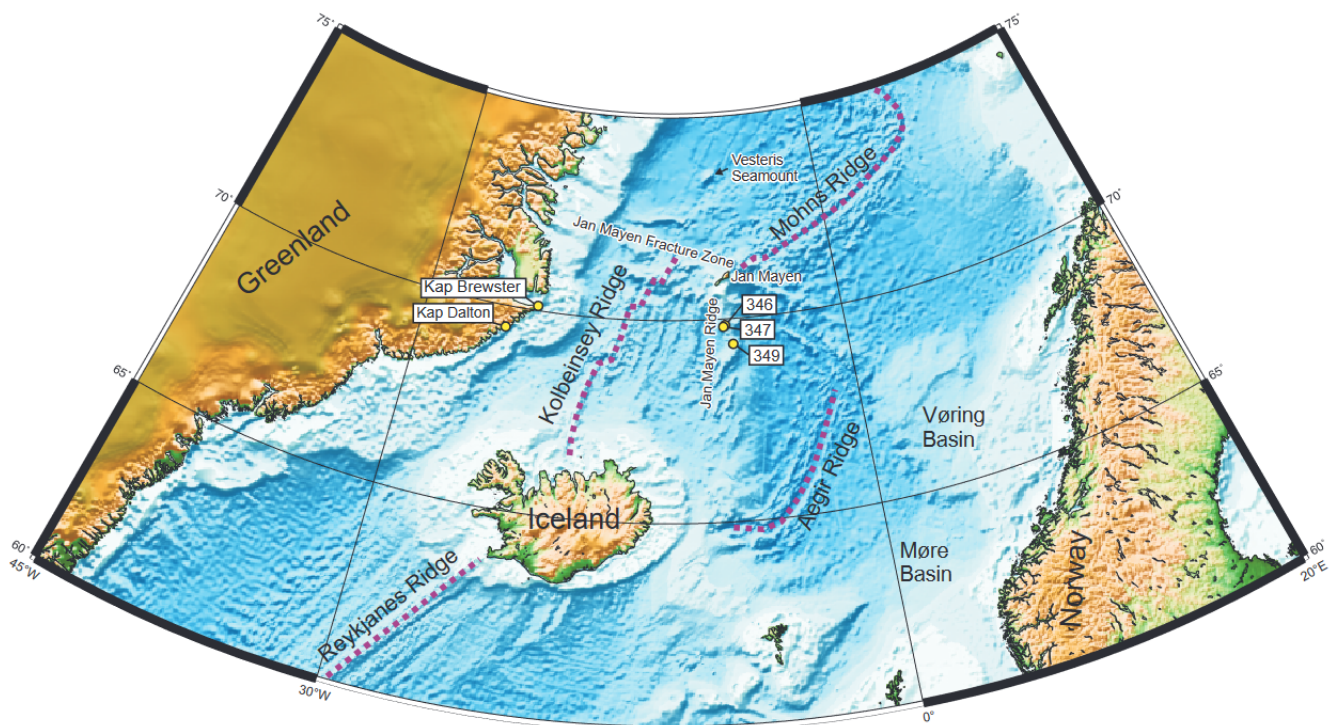


Figure 1. Map of the Norway-Greenland Sea showing the location of Jan Mayen, the three Deep Sea Drilling Project sites discussed in this paper, Kap Brewster and Kap Dalton in East Greenland, and the Vesteris Seamount.

Prior to the opening of the northern North Atlantic in the Early Eocene, what would later become the JMMC lay between the western margin of the Møre Basin and easternmost extremity of Liverpool Land (Figure 2). The eastern margin of the microcontinent was defined in the Early Eocene (chron 24R) when seafloor spreading began on the Aegir Ridge [8]. Rifting then began in the area to the east of what is now Liverpool Land, culminating in seafloor spreading and separation of the microcontinent [1,9–13]. The transition from rifting to seafloor spreading is thought to have been a prolonged and complex process involving the gradual extinction of spreading on the Aegir Ridge from south to north linked to the northward propagation of the Kolbeinsey Ridge, accompanied by the fragmentation of the continental sliver forming the JMMC.

Blischke et al. [14] summarised the present understanding of the breakup history in the vicinity of the JMMC. The first breakup took place along the north-eastern to eastern flank of the JMMC at the start of the Early Eocene, with the emplacement of a series of seaward-dipping reflectors (SDRs) representing the initiation of seafloor spreading along the Aegir Ridge. Towards the end of the Early Eocene, a renewed phase of rifting led to the establishment of a continuous Aegir Ridge spreading system. The second breakup phase, which was focused along the western margin of the JMMC, was initiated in the earliest Oligocene, with a westward shift of volcanic activity along the southern and southwestern parts of the JMMC. Full seafloor spreading as a consequence of the second breakup took place later in the Oligocene, leading to the establishment of the Kolbeinsey Ridge on the western margin of the JMMC, and the cessation of activity on the Aegir Ridge.

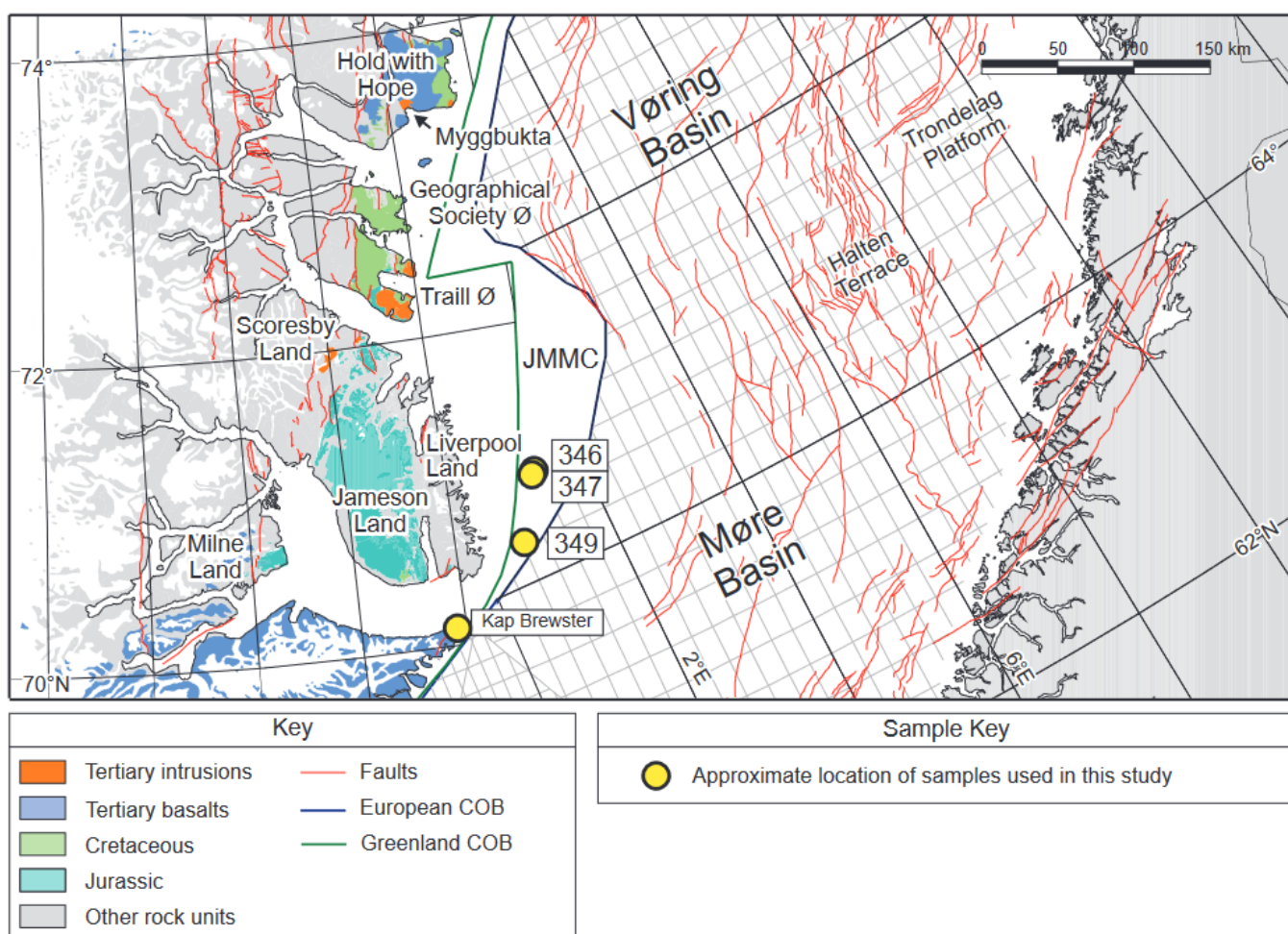


Figure 2. Reconstruction of the Norway-Greenland Sea region, for the time immediately prior to the onset of seafloor spreading in the Paleogene, adapted from Scott [10]. Locations of Deep Sea Drilling Project sites 346, 347 and 349 are only approximate given uncertainties in the reconstructions and the pre-break up shape and location of the Jan Mayen Microcontinent (JMMC). The reconstruction shows the former proximity of the borehole sites to the East Greenland margin. The grid displayed for the eastern part of the area shows Norwegian quadrants and blocks.

A partial record of the time interval believed to cover the formation of the JMMC is provided by the sedimentary successions recorded in Deep Sea Drilling Project (DSDP) boreholes drilled at sites 346, 347 and 349 on the Jan Mayen Ridge (Figure 1) and the post-basaltic sedimentary successions at Kap Brewster in East Greenland (Figures 1 and 2). In this paper, we document the evolution in provenance characteristics during continental breakup at these locations. To place these data in a more rigorous stratigraphic and paleoenvironmental framework, we first discuss and evaluate new biostratigraphic data from these boreholes.

2. Stratigraphy at DSDP Sites 346, 347 and 349, Jan Mayen Ridge

2.1. Summary of Previously Published Information

The succession on the Jan Mayen Ridge was divided into five seismic units by Talwani et al. [15] (Figure 3), the top three of which (Units 1–3) were penetrated at DSDP sites 346, 347 and 349 (Figure 4). Talwani et al. [15] interpreted Unit 5 as pre-Eocene sediments and basement of presumed Caledonian affinity, with the overlying Unit 4 believed to comprise latest Paleocene to Early Eocene basalts.

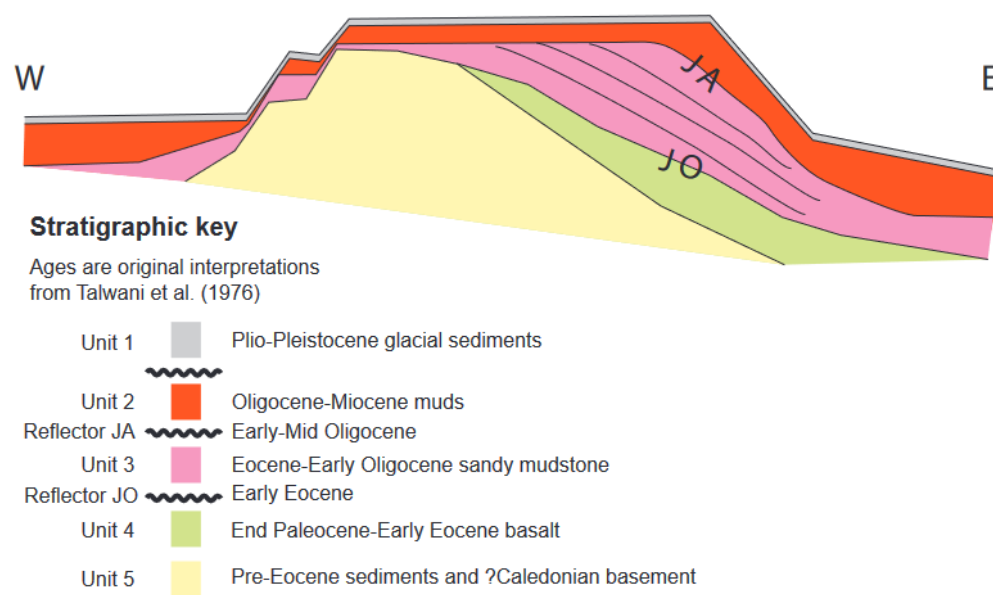


Figure 3. Schematic cross-section of the Jan Mayen Ridge illustrating the geometry of the principal stratigraphic units (after Talwani et al. [15]).

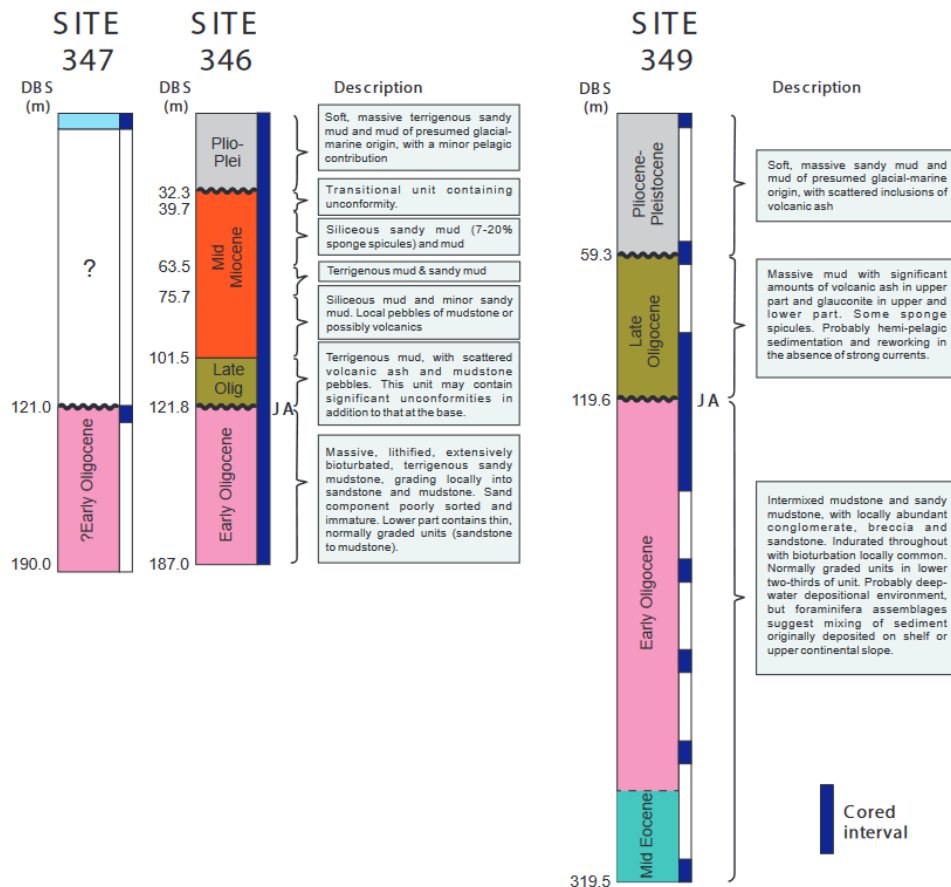


Figure 4. Summary stratigraphic profiles of DSDP Leg 38 sites 346, 347 and 349 after Talwani et al. [15], showing the position of reflector JA, updated with new biostratigraphic data presented herein. DBS = depth below sea floor.

The oldest sediments penetrated by the DSDP boreholes are assigned to Unit 3 (Figure 4). Talwani et al. [15] considered these to be of Oligocene age at Site 346 (>66 m thick) and of Late Eocene–?Oligocene age at Site 349 (>200 m thick). This unit consists of

heavily bioturbated sandy mudstones with occasional normally graded sandstone beds, and at Site 349, rare conglomerate and breccia units. Unit 3 was deposited as part of an eastward-prograding wedge of sediments whilst Jan Mayen was still attached to East Greenland following the onset of seafloor spreading on the Aegir Ridge. The geometry of the Eocene sedimentary wedge (Figure 3) suggests derivation from an area to the west of the Jan Mayen Ridge, in what is now East Greenland. Unit 3 is separated from the underlying Unit 4 by the JO reflector (Figure 3).

Unit 3 is overlain by Unit 2 (60–90 m thick), attributed to the ?Oligocene to Middle Miocene [15]. Units 2 and 3 are separated by seismic reflector JA (Figures 3 and 4), which is associated with a significant increase in consolidation and sonic velocity [15]. Unit 2 consists of sandy mud and biogenic siliceous oozes characterised by a high percentage of sponge spicules, particularly in the lower (?Oligocene) part. Coarse clastic material, including pebbles, is present in the Miocene part, and is possibly of ice-raftered origin. The Middle Miocene part of this unit is well dated using radiolaria and foraminifera, but dating of the ?Oligocene was less certain since it is based on poorly preserved foraminifera and dinocysts [15].

The topmost unit (Unit 1, 32–59 m thick) is composed of soft sandy mud, presumed to be of glacio-marine origin, with interstratified volcanic ash (most likely derived from the island of Jan Mayen itself), and was interpreted to be of Pliocene-Pleistocene age by Talwani et al. [15].

An alternative stratigraphic nomenclature was proposed by Gunnarsson et al. [16] and subsequently adopted by Peron-Pinvidic et al. [17,18]. In this scheme, the interval below the JO reflector is assigned to the SDRs (seaward-dipping reflector series). Above the SDRs, Peron-Pinvidic et al. [17] divided the succession into Unit 1 (Ypresian and earliest Lutetian) at the base, Unit 2 (Lutetian-Rupelian), and Unit 3 (Chattian and younger) at the top. Unit 1 is separated from Unit 2 by the ‘red reflector’, with Unit 3 separated from Unit 2 by reflector JA. DSDP holes 346, 347 and 349 did not penetrate the succession below the ‘red reflector’, which is believed to be a manifestation of plate reorganisation in the Norway Basin during chron C22-21 [17]. Subsequently, Blischke et al. [14] presented a detailed Cenozoic stratigraphic framework for the JMMC, documenting its development from continental breakup to the present day. They defined eleven Cenozoic seismic-stratigraphic units (JM-70 to JM-01) separated by ten unconformities or disconformities, representing the various tectonostratigraphic phases that shaped the JMMC. However, since this paper is specifically focused on the DSDP sites, we have retained the original stratigraphic nomenclature defined by Talwani et al. [15].

2.2. New Palynological Data

The stratigraphy determined by Talwani et al. [15] lacked resolution and was poorly constrained. In order to improve stratigraphic understanding, palynofloral analysis of twenty six samples from sites 346 and 349 on the Jan Mayen Ridge was undertaken. One of the principle outcomes of the new study has been an increase in stratigraphic resolution, with Unit 2 now subdivided into 2a and 2b, and likewise Unit 3 into 3a and 3b (Figures 5 and 6).

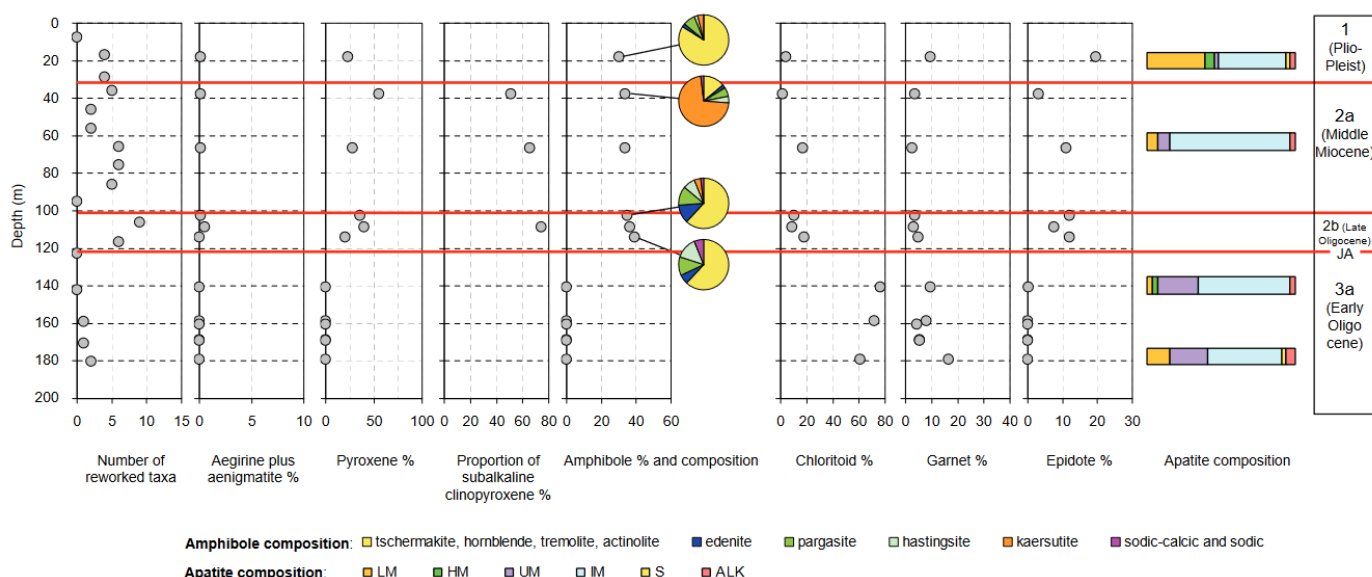


Figure 5. Variations in heavy mineral provenance character and reworked taxa at Deep Sea Drilling Project Site 346. LM = low and medium grade metamorphic and metasomatic, HM = high grade metamorphic, partial melts, leucosomes, UM = ultramafic igneous, IM = mafic igneous including mafic I-type granitoids, S = felsic igneous including S-type and felsic I-type granitoids, ALK = alkaline igneous.

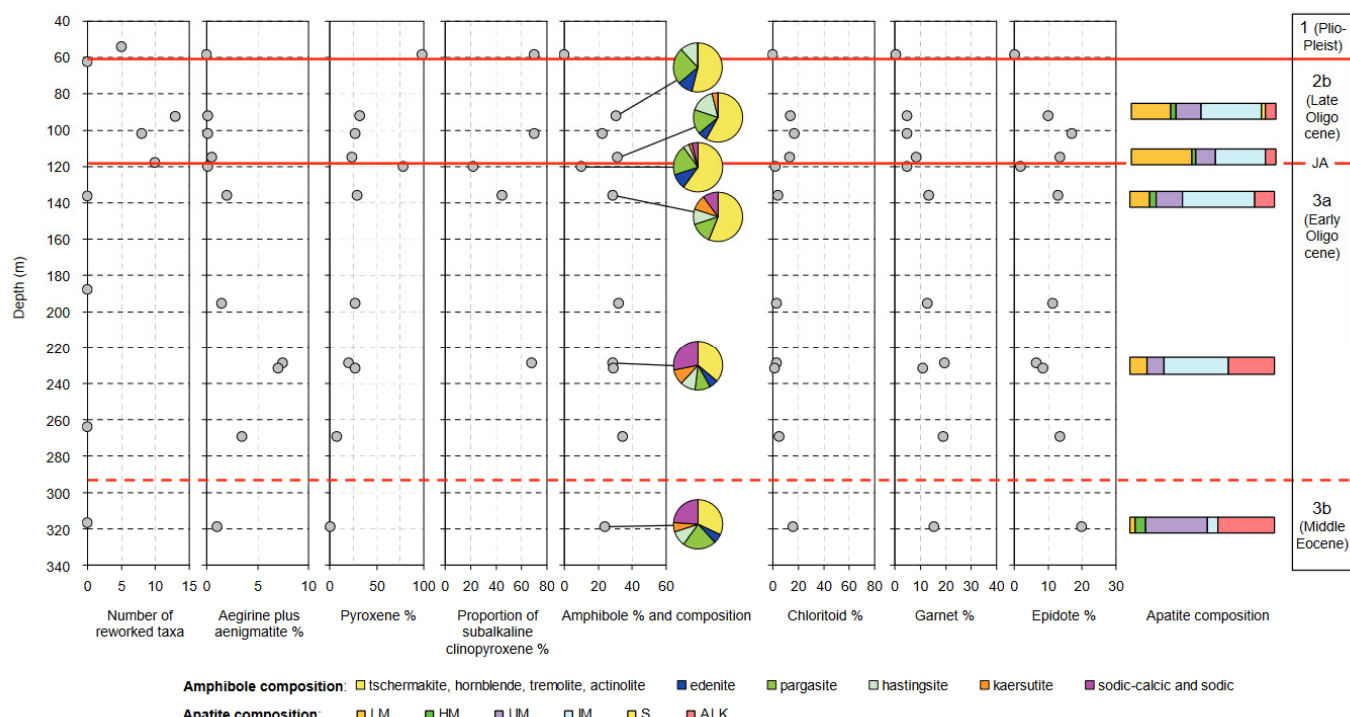


Figure 6. Variations in heavy mineral provenance character and reworked taxa at DSDP Site 349. LM = low and medium grade metamorphic and metasomatic, HM = high grade metamorphic, partial melts, leucosomes, UM = ultramafic igneous, IM = mafic igneous including mafic I-type granitoids, S = felsic igneous including S-type and felsic I-type granitoids, ALK = alkaline igneous.

2.2.1. Unit 3b (Middle Eocene)

A Middle Eocene palynoflora was found in only one sample (Site 349, 316.78 m). The common occurrence of *Areoligera undulata*, *Eatonicysta cf. ursulae*, *Cleistosphaeridium placacanthum*, *Wetzelia articulata* and frequent *Diphyes ficusoides* indicates a mid Middle Eocene age (probably Lutetian), and is comparable to the palynofloras from lowermost Cenozoic

sediments preserved on the East Shetland Platform [19]. The common occurrence of *Wetzelia articulata* is indicative of marine shelf conditions. This is supported by the high frequency of pollen and spores.

2.2.2. Unit 3a (Early Oligocene)

Palynofloras of Early Oligocene age were recorded at both sites 346 and 349. The palynofloras include common specimens of *Phthanoperidinium amoenum*, *P. echinatum*, frequent specimens of *Areoligera semicirculata* and the pollen taxon *Boehlensipollis hohlii*. This palynoflora is characteristic of shallow marine shelf Early Oligocene (Rupelian) sediments, and is similar to that recorded from the East Shetland Platform and the Hebrides Platform [19,20].

The Unit 3a palynoflora is characterised by rich pollen assemblages typical of conifer-fern dominated high latitude forest with associated minor fern mires. This association was transported into a marine environment, most probably by fluvial processes. However, the dinocysts are indicative of shallow shelf marine facies [21] evidenced by the low diversity and high dominance of *Phthanoperidinium* species, which are known to tolerate high levels of environmental stress, in particular lower salinities.

There is no significant reworked component to palynofloral assemblages in this interval. No reworking was recorded at Site 349, with only minor reworking at Site 346. This occurs from 159–180 m and is of probable Early Cretaceous age.

2.2.3. Unit 2b (Late Oligocene)

Palynofloras of Late Oligocene age were recorded at both sites 346 and 349. They include common dinocysts of the taxa *Palaeocystodinium golzowense* and *Cleistosphaeridium placacanthum*, frequent specimens of *Nematosphaeropsis lemniscata* and *N. labrinthea*, *Deflandrea phosphoritica* with common spores of *Cicatricosisporites chattensis* and occurrences of *Tricolporopollenites spinus* pollen. The palynofloras from this interval contain characteristic Late Oligocene assemblages dominated by the coniferous pollen *Pityosporites* spp., occurring with the spores *Deltoidospora adriennis* and *Laevigatosporites haardtii*. Frequent occurrences of *Baculatisporites primarius* and *T. spinus* with *Cicatricosisporites* spp. support a Late Oligocene age assignment. This is verified by the sparse dinocyst flora. Occurrences of the dinocysts *Wetzelia gochtii*, *W. symmetrica* and *Deflandrea phosphoritica* are indicative of an early Late Oligocene age. The dinocyst palynoflora is indicative of deposition in a shallow marine shelfal environment, although the lower abundance of dinocysts at Site 349 suggests a deeper water environment than at Site 346.

Unit 2b is distinctive in containing a highly diverse group of reworked dinoflagellate cysts, pollen and spores, not seen in the underlying intervals. These reworked species are derived from a range of strata from the Carboniferous to the Eocene, particularly Late Namurian-Westphalian, Jurassic, probable Coniacian-Santonian, probable Campanian and Early Eocene (Figures 5 and 6). This influx evidently marks the onset of extensive reworking of the nearby landmass.

2.2.4. Unit 2a (Middle Miocene)

Palynofloras of Middle Miocene age were found at Site 346 but not at Site 349. They are characterized by common specimens of the dinocysts *Palaeocystodinium* sp. Costa & Downie [22], *Selenopemphix* species and *Polysphaeridium zoharii*. They also have a rich miospore component typical of Miocene sediments, containing *Inaperturopollenites hiatus*, *Caryapollenites* spp. and *Momipites* spp., *Nurphar* spp. and *Betula* type suggesting deposition during the Middle Miocene climatic optimum. The microplankton floras are highly variable, a feature indicating that deposition took place over a protracted Middle Miocene period. The occurrences of *Selenopemphix* species and *Palaeocystodinium* sp. Costa and Downie [22] are in accordance with a Middle Miocene age. The palynofloras all indicate deposition in a marine shelf environment. The deepest water facies was recorded at 95.52 m at Site 346, which may represent deposition in a mid shelf environment, with the remainder of the

samples indicating inner to middle neritic facies that experienced a significant input from terrigenous material.

The extent of reworking is lower in the Miocene than in the underlying Oligocene, and is almost absent in the lower part of the Miocene section. The diversity of reworking increases in the upper part of the Miocene section, but does not attain the frequencies seen in the Late Oligocene interval.

2.2.5. Unit 1 (Pliocene-Pleistocene)

Palynofloras of Pliocene-Pleistocene age are found at sites 349 and 346 and include abundant *Spiniferites ramosus* subsp. *ramosus* and common *Operculodinium centrocarpum*. The dinocyst assemblage in these samples is in accordance with a Quaternary marine shelf flora. Due to the small number of samples and the low diversity of the palynofloras, it is not possible to attribute a more specific age. These palynofloras were deposited in a mid neritic marine environment that received significant terrigenous input from the landmass. This landmass was vegetated by a Pinaceae-Cupressaceae-Betulaceae forest with associated ferns and bryophyte mosses. Reworked taxa occur commonly in this interval, with a distribution comparable to that seen in the underlying Miocene.

2.3. Comparison with Previously Published DSDP Ages

There are a number of significant differences between the ages discussed above and those published by Talwani et al. [15]. Unit 3 (which occurs between seismic reflectors JO and JA, see Figures 3 and 4) was ascribed to the Eocene at Site 346 and the Late Eocene-?Oligocene at Site 349 [15]. The lowermost part of this unit (unit 3b) is now dated as Middle Eocene (only penetrated in the lowermost core at Site 349). The remainder of this unit at Site 349 and all of the unit penetrated at Site 346 is now dated as Early Oligocene in age (Unit 3a). Due to the large gaps between the cores at Site 349 (~50 m gap between the sample dated as Middle Eocene and the lowermost Early Oligocene sample) it is not possible to say whether there is a fully conformable section from the Middle Eocene through to the Early Oligocene or whether there is a hiatus within some or all of this time interval.

Unit 2 (between reflector JA and the base “Quaternary”) was originally assigned to the ?Oligocene and Miocene at Site 346 and the ?Oligocene at Site 349. In general these findings have been confirmed. The probable Oligocene section from both wells has been more precisely constrained as Late Oligocene (Unit 2b; Chattian). The probable Miocene section from Site 346 has been confirmed as Middle Miocene (Unit 2a). Similarly, the new palynological data have confirmed the Pliocene-Pleistocene age of the section ascribed to this age by Talwani et al. [15].

2.4. Correlation between Sites 346 and 349

The ages of the sections at sites 346 and 349 are similar, although there are important differences (Figure 7). Strata of Middle Eocene age are present only at Site 349. This is likely to be due to the much deeper penetration of this borehole. There is no reason to believe strata of this age are not present at Site 346, below the terminal depth (TD) of the borehole. Units of Early Oligocene (Rupelian) and Late Oligocene (Chattian) age are present in both boreholes. The boundary between the Early and Late Oligocene corresponds to the boundary between Unit 3a and 2b and coincides with reflector JA. Peron-Pindivic et al. [17] suggest reflector JA is in part diachronous and related to diagenesis (proposed to be the fossilized Opal A to Opal C/T transition), but at least in the vicinity of the DSDP sites it is time-equivalent. The Late Oligocene appears to be significantly thicker at Site 349 (40 m) than at 346 (20 m). Whether this thickness difference is due to differing sedimentation rates or pre-Miocene erosion is unclear. The thick (~70 m) Middle Miocene unit recorded at Site 346 was not identified at Site 349. With Late Oligocene strata recorded at 62.3 m and Pliocene-Pleistocene at 54.3 m, this unit must either be entirely absent or very thin at Site 349. The Plio-Pleistocene section at Site 349 is considerably thicker (59.3 m) than at Site

346 (32.3 m) and it is possible that erosion at the base of the Plio-Pleistocene section may account for the lack of Middle Miocene strata at Site 349.

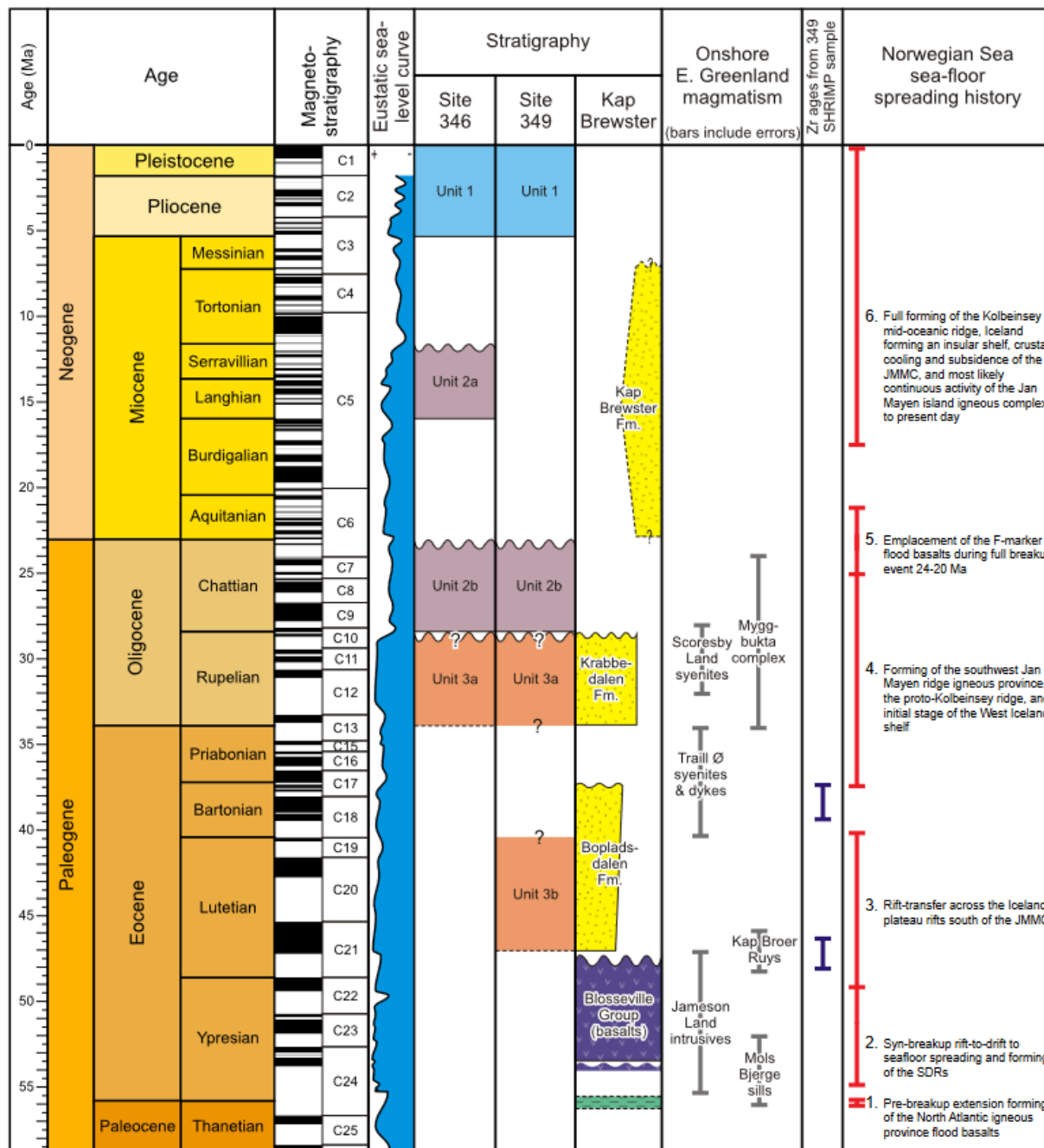


Figure 7. Stratigraphic relationships between Kap Brewster and DSDP sites 346 and 349, compared with igneous events in East Greenland and Greenland-Norway seafloor spreading history. Blosseville Group basalt ages are from Larsen et al. [23] and Storey et al. [24]. East Greenland magmatic events are from Nielsen [25] and Upton et al. [26]. Seafloor spreading history is from Blischke et al. [14].

2.5. Depositional Environment

The palynofloras from the Middle Eocene and Early Oligocene sediments indicate deposition in a marine shelf environment, particularly in the Early Oligocene succession, which appears to represent deposition in a relatively proximal shallow marine setting. This is slightly at odds with the sedimentology, as the sandstone units are thought to have been deposited as turbidites (although deposition as storm units is another possible

interpretation). The high degree of bioturbation is compatible with a shelfal setting. In the Late Oligocene succession, a slightly deeper shelfal setting is indicated by the palynofloras, with water depths somewhat deeper at Site 349 than at Site 346. The palynofloras from the Middle Miocene indicate marine shelf deposition ranging from inner to middle neritic environments, and the Pliocene-Pleistocene succession was deposited in a mid neritic marine environment.

3. Stratigraphy at Kap Brewster, East Greenland

3.1. Summary of Previously Published Information

The Kap Dalton Group, which unconformably overlies the flood basalt succession in East Greenland, consists of a succession of marine sediments over 150 m thick [27–31]. The succession is exposed in two outliers, Kap Dalton and Kap Brewster (Figure 1). The sediments exposed at Kap Brewster (Figure 2) comprise two conformable formations, the Bopladsdalen Formation (80 m) overlain by the Krabbedalen Formation (>100 m). The Bopladsdalen Formation consists of yellow weathering, flaggy sandstones with scattered basalt pebbles, marine and brackish molluscs, and wood with borings. Immediately above the unconformity with the underlying volcanic succession, a 2 m thick conglomerate unit is developed. This conglomerate contains a wide variety of alkaline igneous clasts unrecorded in the underlying Igertiva Formation volcanic succession, which comprises the youngest part of the Blosseville Group and has been dated by the ^{40}Ar - ^{39}Ar method as 49.09 ± 0.48 Ma [23]. The Bopladsdalen Formation has a late Early Eocene age [29]. Soper and Costa [28] assigned an Early Eocene age to the unit on the basis of a limited dinocyst assemblage. ^{40}Ar - ^{39}Ar dating of alkaline basalt clasts at the base of the Bopladsdalen Formation at Kap Dalton revealed ages ranging from 49.17 ± 0.35 Ma to 46.98 ± 0.24 Ma, indicating that deposition commenced no earlier than early Lutetian, ca. 47 Ma [23]. Lava flows within the Bopladsdalen Formation at Kap Dalton have been dated as 43.77 ± 1.08 Ma [23], indicating deposition continued until at least the mid-late Lutetian.

The Krabbedalen Formation, which has a latest Late Eocene-Early Oligocene age based on a diverse assemblage of foraminifera [30], is composed almost entirely of siltstones with concretions and concretionary horizons containing a rich shallow marine macrofauna. Where the formation overlies the Bopladsdalen Formation, the contact is apparently conformable. However, an unconformable contact on basalt is recorded at some other localities and consequently, a hiatus has been suggested between the Bopladsdalen and Krabbedalen formations [30].

3.2. New Palynological Data

Fourteen samples were analysed from the Kap Dalton Group at Kap Brewster (Figure 8). Samples from the basal 70 m of the Bopladsdalen Formation section were either barren or yielded only low diversity palynofloras. Above this, however, the formation yielded a bisaccate pollen dominated palynoflora with a rich pollen and spore component and a more restricted dinoflagellate cyst and algae flora. The age of this part of the Bopladsdalen Formation is best defined by occurrences of common *Deflandrea phosphoritica*, in association with frequent *Spiniferites ramosus* subsp. *ramosus*, frequent *Phthanoperidinium echinatum*, and *Palaeocystodinium golzowense*. Accompanying these are *Minisphaeridium latrictum*, *Cordosphaeridium inodes* and *Glyptostrobus vicina*. This association is characteristic of the latest Early Eocene to early Middle Eocene. The occurrence of *G. vicina* is more suggestive of a basal Middle Eocene age. The age of this part of the succession is further constrained by the pollen and spore flora; the extremely abundant bisaccate pollen is characteristic of the Middle Eocene and younger Paleogene section. During this period, the increasingly cooler, more seasonal climates resulted in changes in vegetation types with increased dominance of seasonal conifer forests. The occurrence of *Sapotaceoidae pollenites* spp. in sample S3593 at the base of the productive section (70 m above the base of the succession) is of importance. This pollen is derived from the Sapotaceae, a family of trees with a subtropical distribution. The occurrence of this taxon at Kap Brewster indicates that during deposition of the basal

part of the productive succession, temperatures at high latitudes were elevated. The only interval in the Middle Eocene where this kind of high latitude temperature was experienced was during the end of the Eocene Thermal Maximum. This was a period of global greenhouse climate that started at around 52.5 Ma and lasted until around 49 Ma, with temperate forests growing up to the polar areas, and mid latitude rain forests. Records of this temperature excursion were found on the East Shetland Platform by Condon et al. [19] at around the Early–Middle Eocene boundary. Therefore, the palynological data are in accordance with the foraminiferal age determinations of Birkenmajer and Jednorowska [30]. The Bopladsdalen Formation therefore equates to Unit 3a (and possibly older sediments) as identified at DSDP Site 349 (Figures 6 and 7).

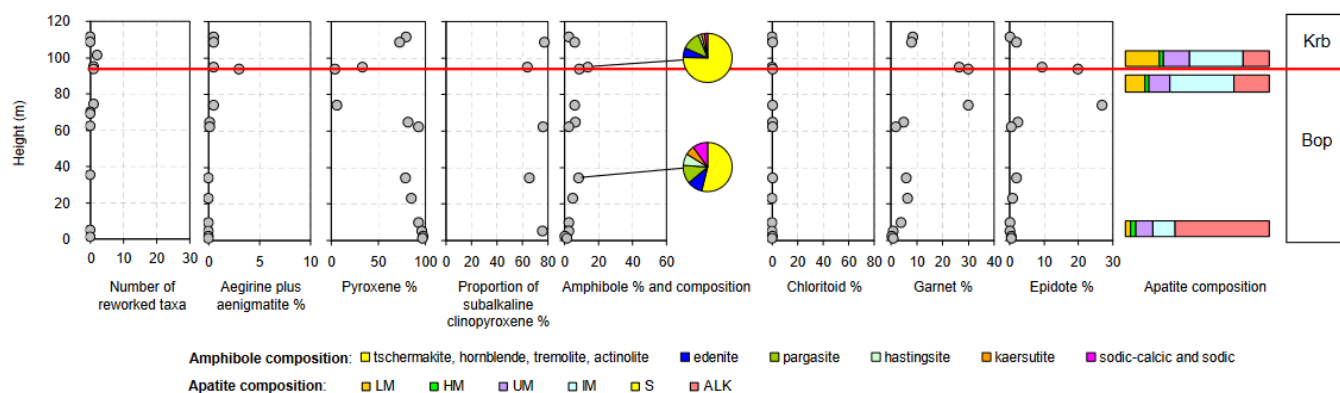


Figure 8. Variations in heavy mineral provenance character and reworked taxa at Kap Brewster. Bop = Bopladsdalen Formation, Krb = Krabbedalen Formation. LM = low and medium grade metamorphic and metasomatic, HM = high grade metamorphic, partial melts, leucosomes, UM = ultramafic igneous, IM = mafic igneous including mafic I-type granitoids, S = felsic igneous including S-type and felsic I-type granitoids, ALK = alkaline igneous.

Palynological examination of two samples from the Bopladsdalen Formation led Soper and Costa [28] to suggest an Early Eocene age based on their dinoflagellate cyst content. Re-examination of sample GGU 179205, described by Soper and Costa [28], proved it to contain a non-diagnostic flora dominated by *Leiosphaera* and *Pterospermella* spp., characteristic of deposition in a low salinity marine environment. The pollen flora includes abundant *Alnipollenites verus*, *Caryapollenites circulus* and *Pityosporites*, common *Nyssapollenites kruschi* subsp. *analepticus*, *Inaperturopollenites hiatus*, *Inratiporopollenites microreticulatus*, and frequent *Caryapollenites veripites*, *Laevigatosporites discordatus* and *Retitricolpites retiformis*. This assemblage is closely comparable to that identified by Condon et al. [19] from late Early Eocene sediments on the East Shetland Platform.

There remains a discrepancy between the biostratigraphic data that indicate deposition of the Bopladsdalen Formation commenced in the latest Early Eocene at Kap Brewster, and ^{40}Ar - ^{39}Ar dating of the basalt pebbles in the basal Bopladsdalen conglomerate at the adjacent Kap Dalton, which is interpreted to indicate deposition did not commence until ca. 47 Ma, some 2 Ma later. It is beyond the scope of this paper to discuss the reasons behind this anomaly.

The Krabbedalen Formation yielded a different palynoflora to the upper Bopladsdalen Formation. Many of the samples yielded very poor assemblages, but the occurrence of *Wetzelia symmetrica* in S3597, 90 m above the base of the succession, is indicative of an Early Oligocene-earliest Late Oligocene age, and the formation therefore equates to Unit 3a in the DSDP holes. The dinocyst *Wetzelia symmetrica* occurs with common pteridophyte spores *Laevigatosporites haardtii* and *Deltoidospora adriennis* and occurrences of *Alnipollenites verus* pollen, typical of the Rupelian floras on the NE Atlantic margin [32]. Taken together with the dinocyst evidence, these terrestrial floras indicate an Early Oligocene age for the Krabbedalen Formation, an age in accordance with the micropalaeontological determinations (Late Eocene to Early Oligocene) of Birkenmajer and

Jednorowska [29]. Soper and Costa [28], who examined three samples from the Krabbedalen Formation, also arrived at the same age determination. These authors recovered a rich dinoflagellate cyst flora including *Areoligera semicirculata*, *Chiropertidium galea* and *Thalassiphora reticulata*, all indicating an Early Oligocene age. A small number of reworked Jurassic palynomorphs are found in the Krabbedalen Formation.

3.3. Depositional Environment

The dinoflagellate cyst floras (including *Deflandrea phosphoritica* and *Palaeocystodinium golzowense*) from the Bopladsdalen Formation are dominated by peridinioid cysts characteristic of shallow marine environments with influences from lowered salinities and turbulence. The occurrence of the gonyaulacoid *Lingulodinium machaerophorum* further indicates that the salinities were lower, as this taxon occupies niches in estuaries and low salinity sea waters [33]. Other gonyaulacoid cysts recorded in this section are common in the shallow water arenaceous sections of the Middle Eocene in southern England and marginal North Sea locations. This group includes *Glyptiphyrocysta vicina*, *Phihanoperidinium echinatum* and *Samlandia chlamydophora* [21,34]. The abundance of pollen and spores in this interval is wholly in agreement with the environmental determination derived from the dinocysts. A shallow marine, turbulent water mass, subject to regular oxidation in the sediment pile (hence the barren section at the base) therefore appears to have been prevalent during the early Middle Eocene. Regional uplift, seen across much of the North Atlantic area during the later Middle Eocene resulted in an unconformity that continued into the Late Eocene. The eustatic sea level rise in the early Rupelian [35] resulted in the resumption of sedimentation in the area, again in shallow water marine conditions, leading to deposition of the Krabbedalen Formation.

4. Heavy Mineral Provenance Signatures

4.1. Analytical Methods

An integrated approach to heavy mineral provenance was adopted in this study. Conventional (petrographic) heavy mineral analysis formed the basic framework, supplemented by major element mineral chemistry on clinopyroxene, garnet and amphibole populations, trace element mineral chemistry on apatite, and a limited programme of single-grain dating by U-Pb on zircon and Ar-Ar on amphibole. Details of analytical methods are provided in the Supplementary Material.

4.2. Heavy Mineral Assemblages

The heavy mineral assemblages in the Eocene-Pleistocene succession on the Jan Mayen margin are diverse, with 22 non-opaque species having been recorded (Table 1). The most abundant minerals are amphibole, chloritoid, clinopyroxene, epidote and garnet, with all other components present in abundances <10% (excluding a single sample with 62% apatite). Some of the minor phases (aegirine, aenigmatite, perovskite and sodic amphibole with the optical properties of arfvedsonite) are particularly significant because they diagnose sediment supply from evolved alkaline igneous rocks such as syenites. Two of these minerals, aenigmatite and perovskite, are extremely scarce as detrital minerals and only rarely have they been previously recorded in sandstones [36–39]. They were identified on the basis of their optical properties, with their presence confirmed by electron microprobe analysis. The presence of highly unstable heavy minerals such as clinopyroxene indicates that the analysed successions have undergone very little diagenetic modification, although there is some evidence for clinopyroxene dissolution in the most deeply buried samples at Site 349, in the form of etched grain surfaces.

Table 1. Relative abundance of non-opaque detrital heavy minerals in samples from the Jan Mayen Ridge Deep Sea Drilling Project (DSDP) sites and CASP samples (S numbers) from Kap Brewster, expressed as frequency % on a count of 200 grains. Ae—aegirine, Ag—aenigmatite, An—andalusite, At—anatase, Ap—apatite, Ca—calcic and sodic-calcic amphibole, Cp—clinopyroxene, Cr—chrome spinel, Ct—chloritoid, Ep—epidote group, Gt—garnet, Ky—kyanite, Mo—monazite, Op—orthopyroxene, Pv—perovskite, Ru—rutile, Sa—sodic amphibole, Sl—sillimanite, Sp—titanite, St—staurolite, To—tourmaline, Zr—zircon. R—rare (<0.5%). The stratigraphic heights of the CASP samples are measured from the base of the Bopladsdalen Formation.

Sample	Ae	Ag	An	At	Ap	Ca	Cp	Cr	Ct	Ep	Gt	Ky	Mo	Op	Pv	Ru	Sa	Sl	Sp	St	To	Zr	
DSDP 346, 18.00 m	R			R	2.0	30.0	21.0	R	4.0	19.5	9.5	1.0	R	2.0		2.0	R	1.5	3.5	1.0	0.5	2.5	
DSDP 346, 37.64 m	R			R	1.5	33.5	55.5		1.5	3.0	3.5	R	R			R	R	1.0	R	R	0.5		
DSDP 346, 66.61 m	R			R	3.5	33.5	27.5	R	17.0	11.0	2.5	1.0	R	0.5		R	R	0.5	1.5	R	0.5		
DSDP 346, 102.60 m	R			R	1.0	35.0	33.5		10.5	12.0	3.5	0.5		2.5		R			1.0	R	R	0.5	
DSDP 346, 108.55 m	0.5				1.5	36.5	40.0		9.0	7.5	3.0	0.5		R		R			1.0	0.5	R		
DSDP 346, 114.10 m					2.5	39.0	19.0		18.0	12.0	5.0	0.5		1.0		R		0.5	0.5	0.5	0.5	1.5	
DSDP 346, 140.60 m				1.0	5.0			R	76.5	R	9.5	R	R				1.5			R	4.0	2.5	
DSDP 346, 158.70 m				2.5	8.0			R	71.5		8.0		R				2.5				0.5	2.5	4.5
DSDP 346, 160.36 m				0.5	6.5			R	80.5		4.5	R	R				0.5			R	3.5	4.0	
DSDP 346, 168.86 m				1.5	3.0			R	81.0		5.5		R				1.5			0.5	R	3.0	4.0
DSDP 346, 169.11 m				1.5	3.0			R	81.0		5.5		R				1.5			0.5	R	3.0	4.0
DSDP 346, 179.18 m				2.0	3.0			R	61.0		16.5		0.5				2.5			0.5	4.5	9.5	
DSDP 347, 122.41 m				1.0	3.5			0.5	R	72.0	0.5	14.0	0.5	R			0.5			2.0	R	2.5	3.0
DSDP 347, 131.28 m				1.0	62.0	R	1.0		27.5	0.5	3.5	R	R				R			1.5		2.0	1.0
DSDP 347, 188.77 m				0.5	9.0			R	82.0		3.0		R				0.5			R	3.5	1.5	
DSDP 349, 58.46 m					0.5	R	98.5				R	0.5										0.5	
DSDP 349, 92.13 m	R				R	1.0	30.5	31.5	R	14.0	10.0	5.0	0.5	R	1.0		1.5	R	1.5	0.5	1.0	2.0	
DSDP 349, 102.10 m	R				R	1.0	22.5	26.0	R	17.0	17.0	5.0	0.5	R	1.5	R	2.0		3.0	1.0	0.5	3.0	
DSDP 349, 114.84 m	0.5				R	1.0	31.5	23.5	R	13.5	13.5	8.5	3.0	R	R	R	0.5	R	1.0	1.0	0.5	0.5	
DSDP 349, 120.00 m	R	R			R	0.5	10.0	78.5	R	2.0	2.0	5.0	1.0	R			0.5	R	R	R	R	0.5	
DSDP 349, 135.90 m	2.0	R		0.5	0.5	28.5	28.5	R	4.0	13.0	13.5	4.0	R	1.0		2.0			1.0	0.5	0.5	0.5	
DSDP 349, 195.50 m	1.5	R		R	2.0	32.0	27.0	R	3.0	11.5	13.0	3.5	R			2.0			2.5	0.5	1.0	0.5	
DSDP 349, 228.92 m	3.5	4.0		R	4.0	28.5	20.5	R	3.0	6.5	19.5	3.5	R			0.5			3.0	1.0	1.0	1.5	
DSDP 349, 231.70 m	3.0	4.0		0.5	R	29.0	27.0	0.5	1.5	8.5	11.0	5.5	1.0				2.5			2.0	1.0	R	3.0
DSDP 349, 269.32 m	2.5	1.0		0.5	4.5	34.5	7.5	R	5.0	13.5	19.0	5.5	R			0.5			2.0	1.5	R	2.5	
DSDP 349, 318.88 m	1.0	R		0.5	5.0	24.0	0.5	0.5	16.0	20.0	15.5	5.0	0.5	R		2.0			3.0	0.5	0.5	5.5	
S3601 (111.5 m)	0.5				R	2.5	80.0	R	R	R	8.5	6.0				0.5			R	2.0	R	R	
S3599 (108.5 m)	0.5				R	6.0	73.0		0.5	2.0	8.0	6.0	R			0.5	R		2.0	0.5	R	1.0	
S3597 (95.0 m)	0.5				R	0.5	14.0	33.5	R	9.5	26.5	5.5	R			R	3.5	R	3.0	0.5	R	3.0	
S3596 (93.6 m)	3.0				R	5.5	9.0	4.0	0.5	0.5	20.0	30.0	10.0	1.5			5.0	0.5		3.5	1.5	0.5	5.0
S3594 (74.0 m)	0.5				3.0	6.0	6.0	R	0.5	27.0	30.0	14.5	R			2.5			3.5	1.5	0.5	4.5	
S3591 (64.6 m)	R				0.5	6.5	82.0		0.5	2.5	5.0	0.5				0.5				0.5		1.5	
S3590 (62.0 m)	R				R	2.5	93.0		0.5	0.5	2.0	1.0				0.5			R		R	R	
S3588 (34.0 m)						8.5	79.0		0.5	2.0	6.0	R				3.0			R			1.0	
S3586 (23.0 m)						5.0	85.5			1.0	6.5	1.0							R	R	R	1.0	
S3585 (9.6 m)					R	2.5	93.0		R	4.0	0.5				R	R	R	R	R	R	R		
S3584 (5.1 m)					R	2.5	96.5	R	R	1.0					R	R	R	R	R	R	R		
S3582 (2.0 m)						0.5	98.0		0.5	0.5	0.5						R	R	R	R	R	R	
S3580 (1.0 m)					R	1.5	97.0			0.5	1.0						R					R	

There are significant variations in heavy mineral characteristics at Site 346 (and the adjacent 347), Site 349 and at Kap Brewster, both in stratigraphic and geographic terms. Stratigraphic variations in key heavy mineral parameters at sites 346 and 349 are shown in Figures 5 and 6, with Kap Brewster summarised in Figure 8.

4.3. Sites 346 and 347

At Site 346, sandstones were analysed from the Early Oligocene (Unit 3a), Late Oligocene (Unit 2b), Middle Miocene (Unit 2a) and Pleistocene (Unit 1). Early Oligocene sandstones with closely comparable compositions were also recovered at the adjacent Site 347, and are therefore considered in conjunction with Site 346.

The Early Oligocene (Unit 3a) assemblages (Figure 5) are unusual in that chloritoid is abundant, comprising between 27% and 82%. Other common phases are apatite (3–9%, excluding one sample from Site 347 with 62%), garnet (3–17%), tourmaline (2–5%) and zircon (1–10%). Anatase and rutile are consistently present in minor amounts. Other phases (amphibole, clinopyroxene, chrome spinel, epidote, kyanite, monazite, staurolite and titanite) are scarce and occur only sporadically. The abundant apatite at 122.41 m from Site 347 is prismatic, unabraded, and clearly of first-cycle origin, most likely representing contemporaneous volcanoclastic input.

The boundary between the Early Oligocene and the Late Oligocene is clearly evident on the stratigraphic plot (Figure 5). Across the boundary, there is a marked reduction in the proportion of chloritoid, in conjunction with major increases in abundance of amphibole and clinopyroxene. Minor amounts of the alkaline indicator mineral aegirine appear in the Late Oligocene, but form only a small part of the heavy mineral assemblages.

The heavy mineral assemblages in the overlying Middle Miocene (Unit 2a) are not dramatically different to those of the Late Oligocene, with amphibole, clinopyroxene, chloritoid, epidote and garnet abundances remaining at similar levels. However, the amphibole in one of the Middle Miocene samples is distinctively deep red-brown in colour, and microprobe analysis indicates this has the composition of kaersutite (Figure 5). The Pleistocene (Unit 1) has a broadly similar heavy mineral assemblage to Units 2a and 2b, although proportions of garnet, epidote and clinopyroxene are somewhat different.

4.4. Site 349

The Site 349 succession includes sandstones of Middle Eocene (Unit 3b), Early Oligocene (Unit 3a), Late Oligocene (Unit 2b) and Pleistocene (Unit 1) age. As at Site 346, there is a change in heavy mineral characteristics across the Early Oligocene–Late Oligocene boundary (Figure 6). Below the boundary, the succession is characterised by high amphibole contents (~30%, apart from the uppermost sample, which has a distinctly lower amphibole content of 10%), and by an upward increase in clinopyroxene abundance from <15% in the Middle Eocene to ~80% at the top of the Early Oligocene. The trend of increasing clinopyroxene may have been accentuated by diagenetic modification, since clinopyroxene shows evidence of greater corrosion with increasing depth. Hence, the low clinopyroxene contents in the Middle Eocene and the lower part of the Early Oligocene may be the result of dissolution and could have been higher prior to burial. Chloritoid contents are relatively low, but are higher in the Middle Eocene than the Early Oligocene. The Middle Eocene–Early Oligocene interval is also distinctive in containing minerals indicative of alkaline igneous sources (aegirine, aenigmatite and sodic amphibole petrographically resembling arfvedsonite), which form >1% of the populations throughout (except in the uppermost sample). These minerals are most abundant in the lower part of the Early Oligocene, where they comprise >3% of the heavy mineral assemblage (Figure 6).

In the Late Oligocene (Unit 2b), clinopyroxene contents drop back to moderate values (~25%), amphibole forms ~20–30%, and there is a distinct increase in chloritoid content. Although alkaline igneous minerals are present, they are less abundant (<1%) than in the Early Oligocene. The heavy mineral assemblage in the single Pleistocene sample (Unit 1) is markedly different to the underlying sandstones, consisting almost exclusively of clinopyroxene.

4.5. Kap Brewster

The succession analysed at Kap Brewster comprises the Bopladsdalen Formation (equivalent to Unit 3b and possibly older) overlain by the Krabbedalen Formation (equivalent to Unit 3a). The lower and middle parts of the Bopladsdalen Formation are dominated by clinopyroxene, which forms 79–98% of the heavy mineral assemblages (Figure 8). The only other minerals to form a significant proportion of the assemblages are amphibole and garnet (8.5% and 6.5%, respectively). Minerals indicative of alkaline igneous activity are scarce in this interval.

The upper two Bopladsdalen Formation samples show a distinct change in provenance characteristics, with clinopyroxene contents much reduced (<10%) and non-magmatic (metamorphic) sources much more in evidence. Garnet is the most abundant mineral, with epidote and kyanite also forming >10% of the assemblages. Alkaline igneous indicator minerals (aegirine and arfvedsonite) are present in small amounts.

There is a further change in provenance at the base of the Krabbedalen Formation, manifested by renewed abundance of clinopyroxene (33%). Clinopyroxene contents continue to

rise through the Krabbedalen Formation, culminating with a value of 80% immediately below the Miocene (Figure 7).

4.6. Mineral Chemistry

4.6.1. Clinopyroxene

The majority of the clinopyroxenes analysed in this study have augitic-salitic compositions (Figure 9), typical of basaltic parentage. There are only two samples that deviate significantly from these compositions. The sample from the top of Unit 3a at Site 349 (119.55 m) shows a well-defined Fe-enrichment trend typical of fractionation, indicating that some of the clinopyroxenes in this sample were derived from more evolved magmatic rocks. The Pleistocene (Unit 1) sample from Site 349 has a bimodal population, with some grains having augitic-salitic compositions and others being more ferroan (Figure 9).

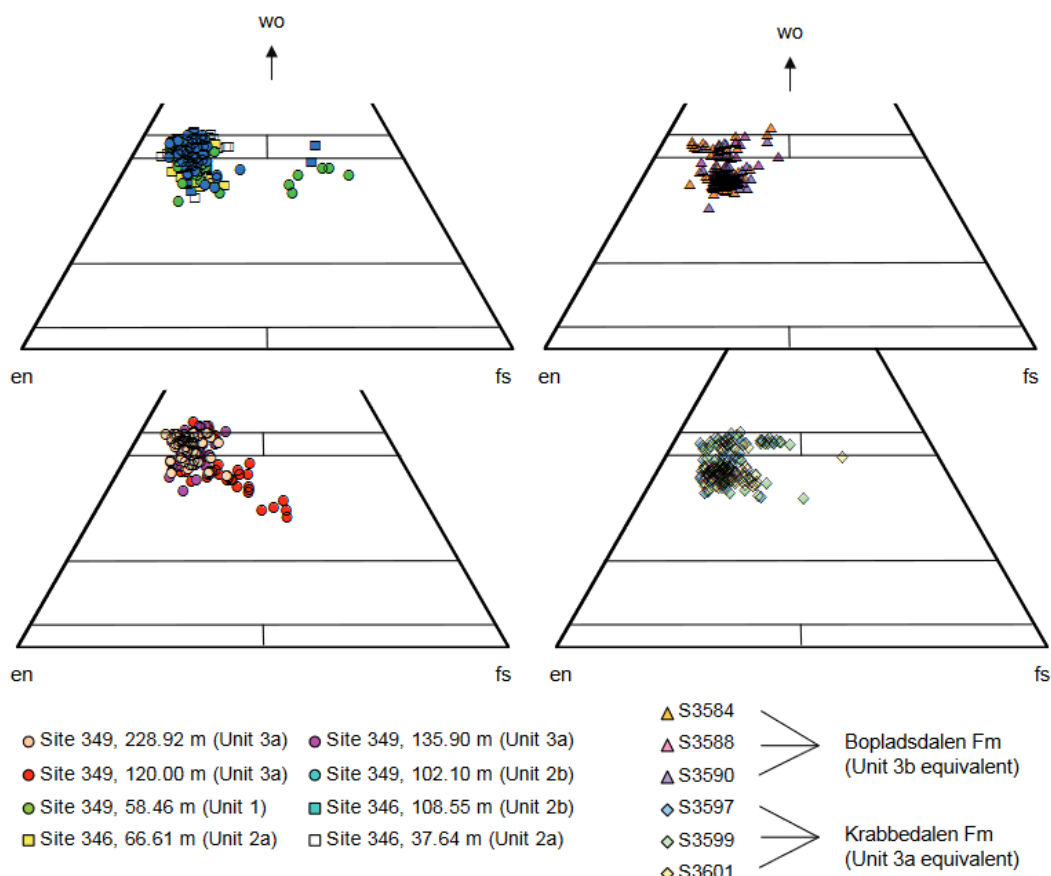


Figure 9. Clinopyroxenes from Deep Sea Drilling Project sites and Kap Brewster plotted on wo (wollastonite)—en (enstatite)—fs (ferrosilite) ternary diagrams [40].

On the basis of the $\text{SiO}_2\text{-Al}_2\text{O}_3$ diagram [38], distinct differences in the relative abundance of subalkaline and alkaline clinopyroxenes can be seen within the data set (Figure 10). The clinopyroxenes in Unit 3a at Site 349 appear to show a stratigraphic trend, with alkaline grains becoming more abundant higher in the section (Figure 6), culminating with the sample at 119.55 m, which, as discussed above, also shows the greatest degree of fractionation (Figure 9). This trend is reversed across the Unit 3a/2b (Early/Late Oligocene) boundary, with an increase in the abundance of subalkaline grains in the Late Oligocene (Figure 6), a feature that persists into the Pleistocene. Clinopyroxene geochemistry therefore provides additional evidence for a change in provenance across the Early/Late Oligocene boundary.

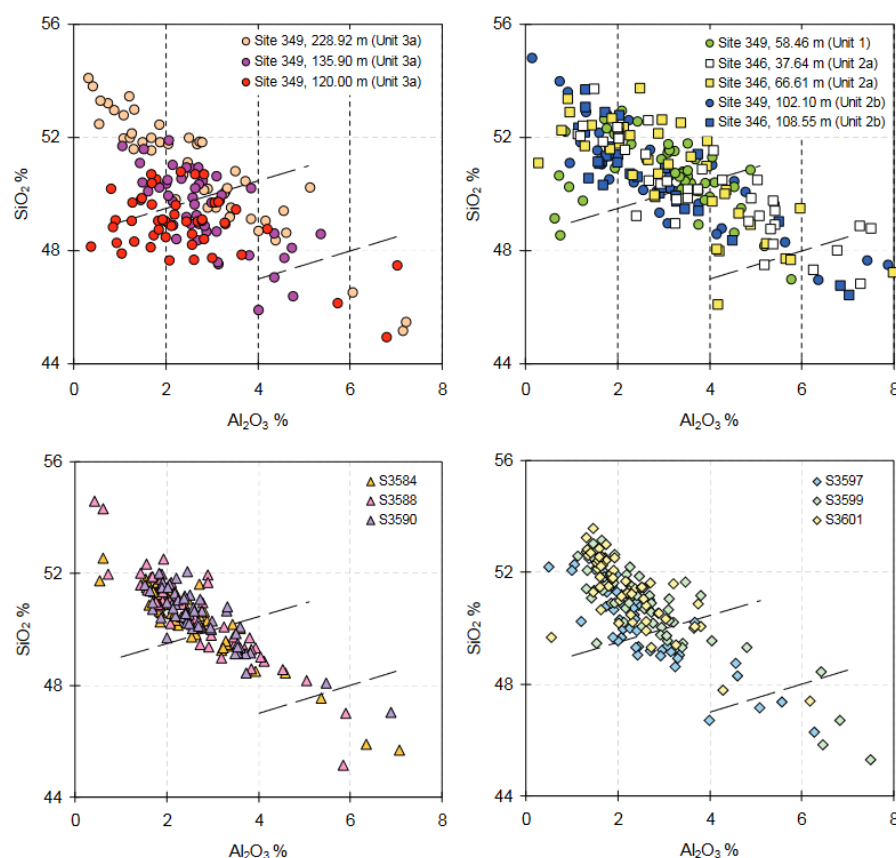


Figure 10. Clinopyroxenes from Deep Sea Drilling Project sites and Kap Brewster plotted on $\text{SiO}_2\text{-Al}_2\text{O}_3$ diagrams of LeBas [41]. Kap Brewster samples S3584, S3588 and S3590 are from the Bopladsdalen Formation and S3597, S3599 and S3601 are from the Krabbedalen Formation.

At Site 346, clinopyroxene appears in significant amounts only above the Early/Late Oligocene boundary (Figure 5). In Unit 2b, grains have predominantly subalkaline compositions similar to those found in the equivalent unit at Site 349, as do those in the lower part of the overlying Unit 2a. However, the shallower of the two samples analysed from Unit 2a (37.64 m depth) contains a higher proportion of alkaline grains. This sample also differs in having higher clinopyroxene contents and abundant kaersutitic amphibole (Figure 5).

Clinopyroxene populations in both the Bopladsdalen and Krabbedalen formations of Kap Brewster are richer in subalkaline types compared with those on the Jan Mayen Ridge (Figure 10), especially when compared with Unit 3a. The data therefore indicate that the clinopyroxenes supplied to the Kap Brewster area had a different source to those supplied to the Jan Mayen Ridge during the Early Oligocene.

4.6.2. Garnet

Garnet populations (Figure 11) contain two main components, a high-Mg, low-Ca group and a low-Mg, variable Ca group (Types A and B in the terminology of Morton et al. [38]). Type C (high-Mg, high-Ca) garnets are minor and Type D ($\text{Fe}^{3+}\text{-Ca}$) are scarce. Consequently, variations in garnet geochemistry can be displayed using a plot of Type A vs. Type B (Figure 11). This diagram displays a distinct difference in garnet provenance between the Kap Brewster section and the sites on the Jan Mayen Ridge. Both the Bopladsdalen and Krabbedalen formations have higher Type A garnet contents than all samples from the Jan Mayen Ridge. The Jan Mayen Ridge samples have low abundances of Type A garnet, except for one Early Oligocene sample from Site 349, suggesting a possible provenance link with the Kap Brewster area at this level. The same is true of the Pleistocene sample in Site 346. There is a slight reduction in abundance of Type A garnet across

the Early/Late Oligocene boundary at both of the Jan Mayen Ridge sites, confirming the conventional heavy mineral evidence for a change in provenance across this boundary.

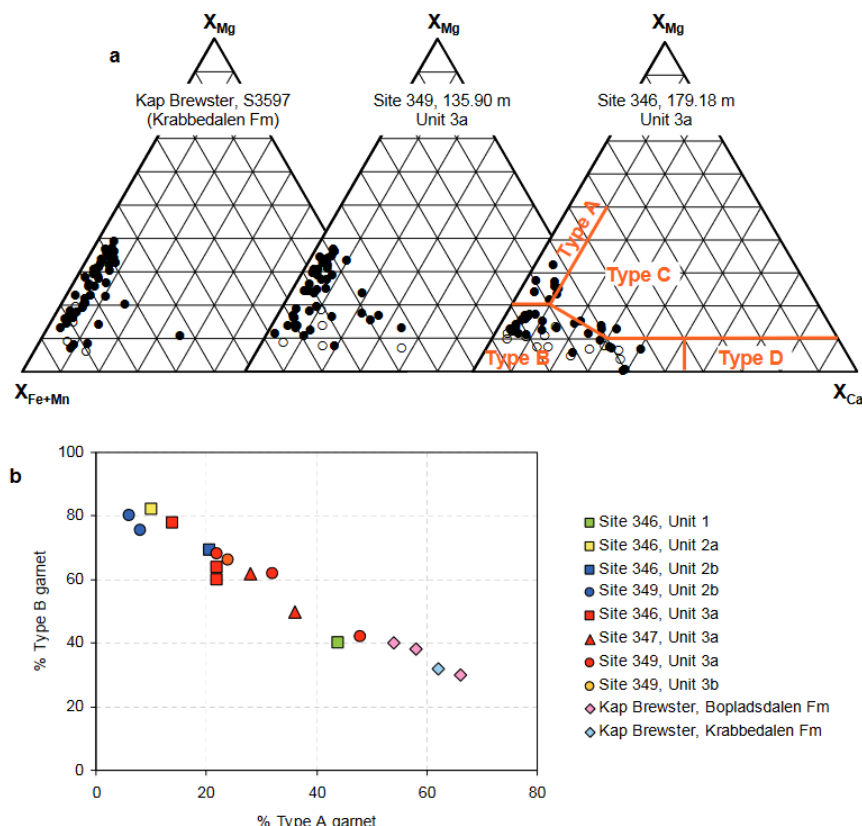


Figure 11. (a) Representative ternary plots of garnet compositions from the Jan Mayen Ridge and Kap Brewster. Fields A, B and C are as defined by Morton et al. [42]. X_{Fe} , X_{Mg} , X_{Ca} , X_{Mn} = proportions of Fe, Mg, Ca and Mn in the garnet formula with all Fe calculated as Fe^{2+} . ●— $X_{Mn} < 5\%$. ○— $X_{Mn} > 5\%$. (b) Relative abundance of garnet types A and B in sandstones from the Jan Mayen Ridge and Kap Brewster.

4.6.3. Amphibole

The Eocene-Pleistocene successions at the Jan Mayen DSDP sites and Kap Brewster are characterised by a wide variety of amphibole compositions, including calcic amphiboles (tremolite- actinolite, hornblende, tschermakite, pargasite, edenite, hastingsite and kaersutite), together with sodic-calcic (kataphorite and richterite) and sodic types (eckermannite and arfvedsonite). Variations in the relative abundance of these amphibole types are shown in Figures 5, 6 and 8.

The Middle Eocene and Early Oligocene succession at Site 349 (units 3b and 3a) is distinctive in containing abundant sodic-calcic amphibole, in conjunction with kaersutite, these amphiboles becoming less abundant above the Early/Late Oligocene boundary. This pattern ties in with the distribution of other alkaline indicator minerals (aegirine and aenigmatite), which also characterise the Middle Eocene to Early Oligocene succession at Site 349 and which become less abundant higher in the section (Figure 6). The change in amphibole composition provides further evidence for a change in provenance at the Early/Late Oligocene boundary.

The amphiboles at Site 346 (units 2b, 2a and 1) are generally similar to those in Unit 2a at Site 349, being dominated by calcic amphiboles. However, the shallower of the two Middle Miocene samples has a distinctive amphibole suite dominated by kaersutite. The amphiboles in this sample have been dated by single step laser fusion $^{40}\text{Ar}/^{39}\text{Ar}$. Apart from two grains with Early Paleozoic ages at c. 420 Ma, evidently representing derivation from Caledonian-age basement, there appears to be two groups of kaersutite in the sample

(Figure 12). Isochron plots (Figure 12) indicate that the larger group, which comprises 7 grains, has an age of 22.2 ± 0.4 Ma with an MSWD of 0.35 (Early Miocene). These grains therefore predate the sediment. The smaller group (comprising 3 grains) has an age of 10.3 ± 0.8 Ma with an MSWD of 0.0025 (Middle-Late Miocene), essentially coeval with the biostratigraphic age data. These data therefore provide evidence for magmatic activity in the vicinity of Jan Mayen during the Early and Middle Miocene.

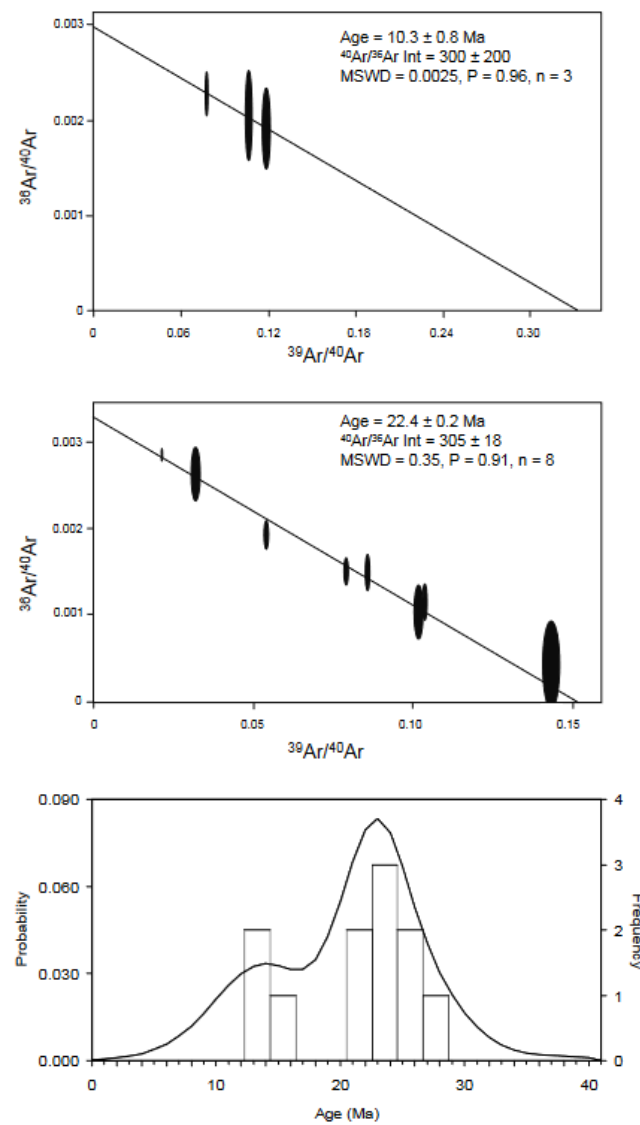


Figure 12. Isochron diagrams and probability distribution ages of kaersutitic amphibole in the sample from 37.64 m at Site 346 (Middle Miocene, Unit 2a).

4.6.4. Apatite

Apatite can be derived from both igneous and metamorphic lithologies, and compositions of detrital apatite can be utilised as a guide to their source [43,44]. Igneous apatites can be differentiated from those of metamorphic origin using a number of criteria [43,45]. In this study, the affinities of the apatites have been assessed using the plot of Sr/Y vs. total light rare earth element (LREE) contents (Figure 13) as devised by O'Sullivan et al. [45].

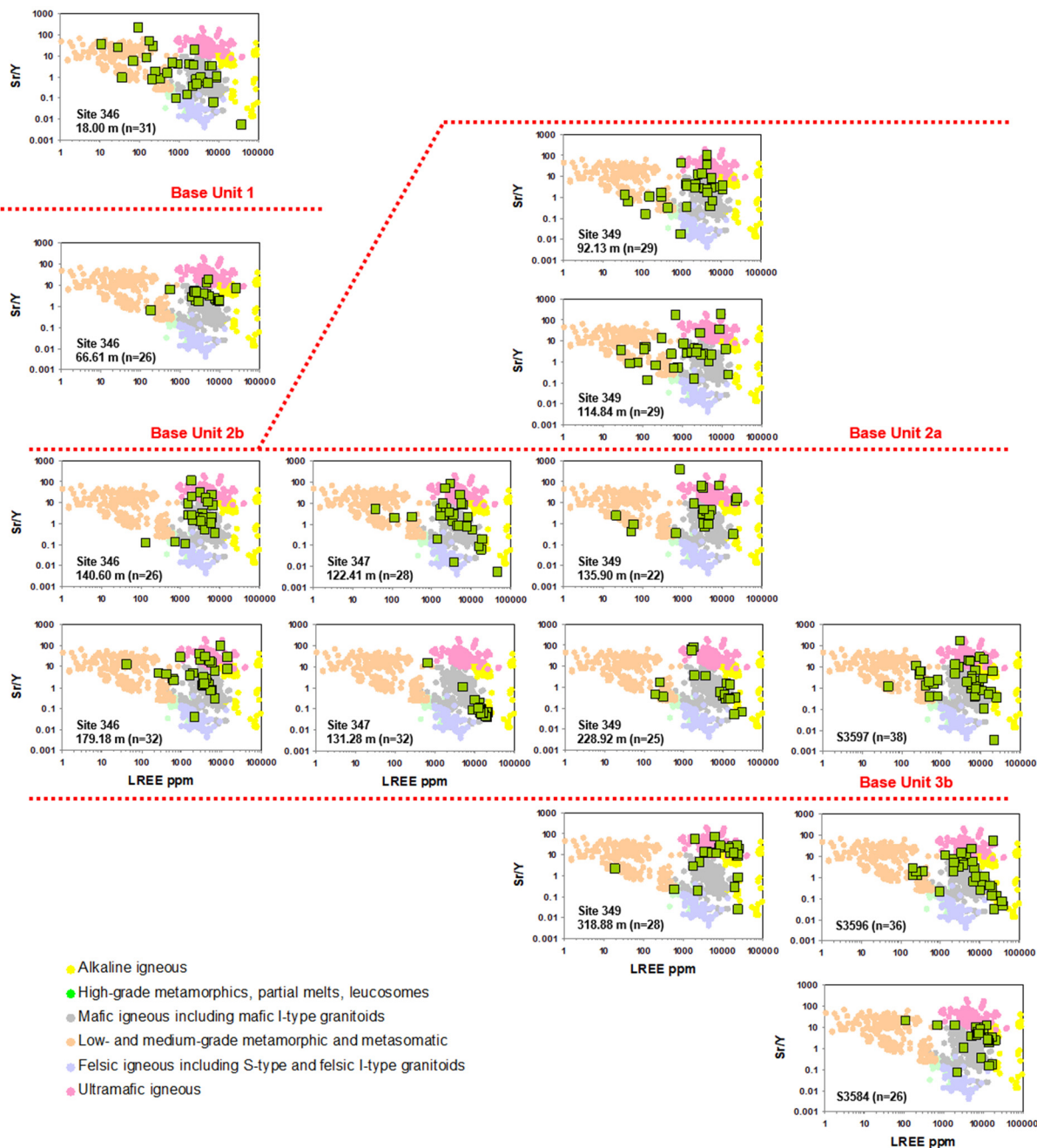


Figure 13. Detrital apatite compositions from the Jan Mayen Ridge and Kap Brewster plotted on the Sr/Y-LREE diagram of O’Sullivan et al. [45], showing the range of stratigraphic and regional variations in apatite provenance.

There are clear changes in apatite provenance at the DSDP sites. At sites 346 and 347, Unit 3a (Early Oligocene) is dominated by mafic igneous apatite, with subordinate ultramafic varieties and minor metamorphic types. The sample from Site 347 with abundant prismatic first-cycle apatite (131.28 m), by contrast, has a closely clustered group of compositions that correspond to alkaline igneous compositions. The sample from Unit 2a (Middle Miocene) is again dominated by mafic apatites, which for the most part form a tight cluster on the plot. The Unit 1 (Pleistocene) sample has a much more diverse suite, with metamorphic varieties being significantly more abundant than in the older part of the succession. At Site 349, the Middle Eocene (Unit 3b) sample is rich in alkaline and ultramafic apatite. Mafic apatite becomes more important in Unit 3a (Early Oligocene), al-

though ultramafic and alkaline types remain conspicuous. Above the Early/Late Oligocene boundary, there is a distinct increase in the abundance of metamorphic apatites.

At Kap Brewster, the basal Bopladsdalen Formation has a large group of alkaline igneous apatites, consistent with the presence of alkaline igneous clasts at this level in Kap Dalton [23]. Alkaline apatites remain common but are reduced in number in the upper Bopladsdalen and Krabbedalen, which have more diverse igneous apatite suites including mafic and ultramafic varieties. In addition, metamorphic apatites become more common towards the top of the succession.

4.6.5. Zircon

U-Pb dating was conducted on the Middle Eocene (Unit 3b) sample at 314.39 m in DSDP Site 349. The age spectrum (Figure 14) is relatively complex, with several clusters separated by intervals with little age representation. There is an Archaean group (c. 2600–2950 Ma), comprising 8 zircons (~15% of the population), then an interval between 2600 Ma and 2050 Ma with comparatively little representation. Mid-Proterozoic (c. 1000–2050 Ma) zircons comprise ~63% of the population (34 zircons). This group is polymodal, with three apparent clusters, one from c. 1800–2050 Ma, one at c. 1650 Ma, and one from c. 1000–1450 Ma. There are six Early Paleozoic grains (11% of the population), corresponding to the Caledonian orogeny, two Cretaceous (Aptian) grains (115 Ma and 120 Ma) and two grains dated as Eocene (39 Ma and 47 Ma).

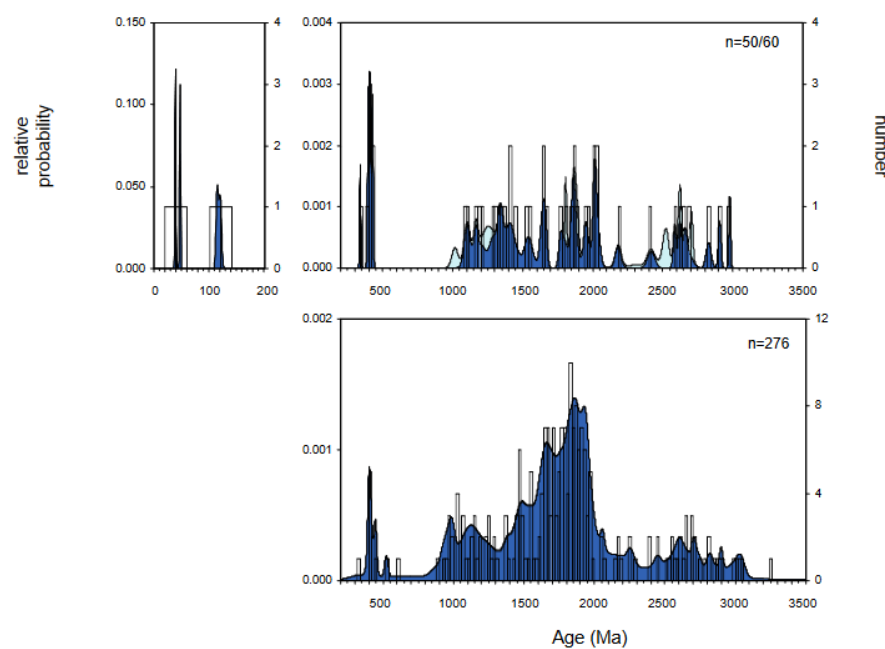


Figure 14. Upper diagram is a probability density plot of zircon ages in a Middle Eocene sample from Site 349 (314.39 m depth) determined by SHRIMP. Dark blue areas are zircons with <10% discordance, pale blue areas are zircons with >10% discordance. ‘n’ is number of zircons with <10% discordance in the total zircon population. Lower plot shows zircons from samples of Late Oligocene volcaniclastic sandstones dredged from the western Jan Mayen Fracture Zone.

Detrital zircon age data are also available for the Late Oligocene succession, in this case from sandstones dredged from the Jan Mayen Fracture Zone (Figure 1). The three analysed samples yielded similar age distributions [46] and the combined U-Pb ages are shown in Figure 14 for comparison with the Eocene sample. The overall age spectra are closely comparable, but Palaeoproterozoic to Early Mesoproterozoic zircons are more abundant in the Late Oligocene.

5. Discussion

The systematic changes in provenance characteristics in sandstones from the Middle Eocene and younger sedimentary successions at DSDP sites 346, 347 and 349, together with the succession at Kap Brewster, are related to events during the separation of the JMMC from East Greenland (Figure 7). The key criteria are: (i) a major increase in the variety, age range and abundance of reworked palynomorphs between Unit 3 (Middle-Eocene-Early Oligocene) and Unit 2 (Late Oligocene-Miocene); (ii) a change in heavy mineral provenance character across the Unit 3/Unit 2 boundary at sites 346 and 349; (iii) at Site 346, predominantly metasedimentary assemblages (dominated by chloritoid and garnet) in Unit 3 give way to mixed metamorphic/igneous assemblages richer in clinopyroxene, epidote and calcic amphibole in Unit 2; and (iv) at Site 349, the Unit 3 assemblages are predominantly igneous (clinopyroxene, mafic/intermediate and alkaline apatite, sodic/calcic and sodic amphiboles), with the overlying Unit 2 having greater metamorphic character (calcic amphibole, epidote, chloritoid), although igneous components remain important.

The existence of lateral differences in provenance character in Unit 3 indicates that there were two distinct transport systems operating in the area, one supplying the area sampled by sites 346 and 347, and the other supplying the area sampled by Site 349. In Unit 2, however, provenance characteristics at the two sites show marked convergence (Figure 15).

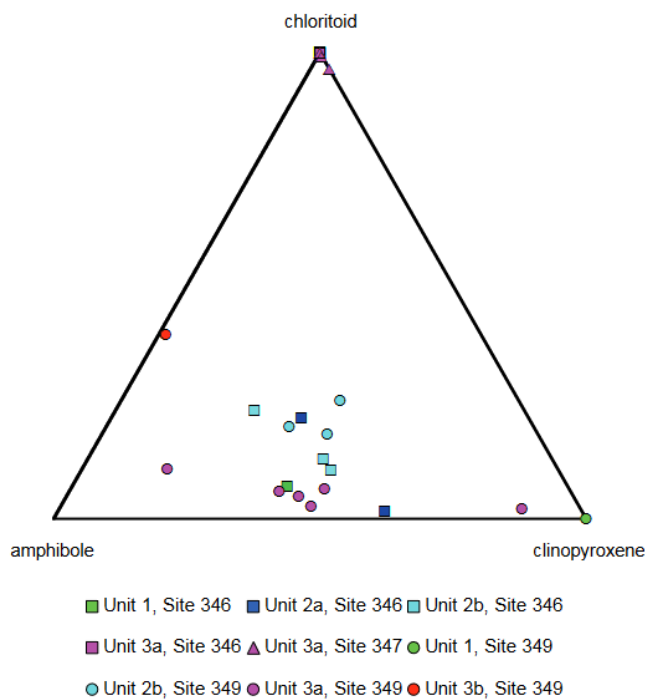


Figure 15. Ternary diagram demonstrating the convergence of heavy mineral assemblage compositions from the Early Oligocene (Unit 3a) to the Late Oligocene (Unit 2b) at the Jan Mayen Ridge sites.

5.1. Middle Eocene to Early Oligocene

The system operative at sites 346 and 347 supplied sediment derived from chloritoid-rich metasedimentary basement rocks. The only evidence for input from magmatic sources at these locations comes from apatite geochemistry, which indicates detrital input predominantly from mafic igneous rocks. There is also evidence for air-fall pyroclastic apatite derived from an alkaline source, witnessed by abundant prismatic first-cycle grains in one of the samples from Site 347 (131.28 m). The origin of the chloritoid-bearing sediment remains enigmatic, but must lie within the metasediments of the Eleanore Bay Supergroup or their lateral equivalents. A regional study of heavy mineral assemblages in moraine and outwash samples derived from East Greenland [47] failed to identify any areas cur-

rently supplying chloritoid, suggesting that more local basement on Jan Mayen might have been responsible. However, East Greenland cannot be ruled out since distances between moraine/outwash sampling stations were inevitably large and it is possible that chloritoid-bearing metasediments were unsampled. Chloritoid has not yet been reported from East Greenland metasediments [48], and although it is known from Nansen Land, in the far northwest of Greenland [49], this is an unfeasibly long distance from the JMMC.

By contrast, the system that deposited sediment at Site 349 was derived from an area that included metamorphic basement (sourcing phases such as garnet, kyanite, staurolite and some of the amphiboles), together with magmatic sources that supplied phases such as clinopyroxene, kaersutite, sodic-calcic amphibole, aegirine, aenigmatite, arfvedsonite, perovskite, and apatite of alkaline, mafic and ultramafic origin. Zircon age data from a Middle Eocene sample indicates that much of the zircon is derived from Early Paleozoic, mid-Proterozoic and Archaean sources, but the two Eocene grains demonstrate input from penecontemporaneous magmatic rocks. Apart from the two Eocene zircons and two Early Cretaceous zircons, the zircon ages correspond to crust-forming events recorded in other Paleozoic and Mesozoic sandstones of East Greenland [46,50] and in modern moraine/outwash samples from the same region [47]. The presence of Aptian zircons indicates that at least some of the sediment must have been recycled from mid-Cretaceous or younger sandstones such as those presently exposed on Traill Ø and Geographical Society Ø on the adjacent East Greenland landmass [51]. The relatively low abundance of chloritoid indicates that the metasedimentary source supplying sites 346 and 347 had little influence at Site 349.

The igneous components in the Middle Eocene to Early Oligocene succession at Site 349 provide evidence for evolution in the nature of the magmatic source during this interval. The key observations are: (i) an upward decrease in the abundance of alkaline indicator minerals, including aegirine, aenigmatite and arfvedsonite, sodic-calcic amphiboles, and alkaline apatites, indicating that alkaline magmatic rocks became less important with time; (ii) an upward increase in the abundance of clinopyroxene and mafic apatites, indicating an increase in supply from mafic sources; and (iii) an upward increase in the abundance of alkaline clinopyroxene, together with evidence for increasing fractionation, suggesting that although mafic sources became more important with time, the degree of partial melting and magma supply rates decreased towards the top of the early Oligocene.

There is abundant evidence for magmatic activity during the Middle Eocene to Early Oligocene onshore East Greenland adjacent to the JMMC (Figure 7), including alkaline rocks (syenites and dykes on Traill Ø and syenites in Scoresby Land) and mafic rocks of the Myggbukta Complex [25,26]. The combination of input from metamorphic basement rocks and contemporaneous alkaline and mafic magmatic rocks indicates that the source area lay on the adjacent part of East Greenland. The mineralogical data therefore suggest that at this time, this part of the Jan Mayen Ridge was still attached to East Greenland, allowing sediment to be transferred from this landmass to the eastern margin of the JMMC. The evolution in magmatic activity as indicated by the heavy mineral assemblages suggests there was an increase in the extent of partial melting during the Middle Eocene to Early Oligocene, followed by a decrease in magma supply rate very near the top of the interval. The observed evolution is consistent with a period of rifting between the Jan Mayen Ridge and East Greenland during the Middle Eocene to Early Oligocene interval.

In East Greenland, the early part of the Middle Eocene interval (Bopladsdalen Formation) is dominated by clinopyroxene, predominantly of subalkaline composition. The source of this detritus is interpreted to be the Blosseville Group basalts, which have predominantly subalkaline affinities. There are subordinate alkali basalts, such as those of the Prinsen af Wales Bjerge Formation [52], which could have supplied the alkaline apatites, although alkaline plutonic rocks such as the Gardiner Complex in the Kangerlussuaq region [25] are also possible sources. Towards the top of the Bopladsdalen Formation, the major influx of non-volcanic heavy minerals (especially garnet, epidote and kyanite) indicates that at this time, the sediment source was inland, beyond the western extent of

the main basalt pile. The change from local basaltic input to more distal metamorphic (or recycled sedimentary) sourcing is interpreted as the result of a relative sea level rise that inundated the local basaltic terrain, also indicated by the change in depositional environment from fluvial to shallow marine. Alkaline indicator minerals (aegirine, arfvedsonite) are also relatively common in this part of the Middle Eocene, similar to the situation at Site 349. It is also noteworthy that the Middle Eocene at Site 349 has similar heavy mineral assemblages and apatite compositions to the upper part of the Bopladsdalen Formation (compare Figures 6 and 8), suggesting that the two sites may have had a common provenance at this time.

The overlying Early Oligocene Krabbedalen Formation shows an overall upward increase in clinopyroxene, indicating a gradual return to sourcing from mafic rocks. The clinopyroxenes are again predominantly of subalkaline parentage, contrasting with the clinopyroxenes in the equivalent Unit 3a at Site 349. The reappearance of abundant clinopyroxene suggests that the Blosseville Group basalt pile was once again exposed. The increase in clinopyroxene content is accompanied by an abrupt fining of grain size and increased water depths. Tectonic uplift, in the context of the extensional regime related to the separation of the JMMC, is the most likely explanation, with normal faulting resulting in footwall uplift and exposure of basalts, and hanging wall subsidence resulting in increased water depths. The alternative possibility is that the basalt pile was exposed due to sea level fall, but this would most likely be accompanied by an increase in grain size as facies belts prograded into the basin, together with a change to shallower water or even continental depositional environments, neither of which are seen. The contrast in detrital mineral compositions (clinopyroxene, amphibole, garnet and, to a lesser extent, apatite) between Kap Brewster and Site 349 indicates that at this time, the areas were supplied by different transport systems.

5.2. Late Oligocene

The major change in provenance at the Early/Late Oligocene boundary marks the end of contrasting mineralogy between the two parts of the Jan Mayen Ridge, with assemblages at both sites having closely comparable characteristics in younger rocks. For the most part, the Late Oligocene assemblages appear to be intermediate between the chloritoid-rich sandstones found in the Early Oligocene at sites 346 and 347, and the clinopyroxene-, amphibole- and garnet-rich sandstones in the Early Oligocene from Site 349 (Figure 15). On this basis alone, the Late Oligocene sandstones could be reworked from the Early Oligocene on the Jan Mayen Ridge. However, the provenance change at the Early/Late Oligocene boundary coincides with a large increase both in the number of reworked palynomorphs and the age range of the reworked taxa (Figures 5 and 6). The reworked species are derived from a wide range of strata from the Carboniferous to the Eocene (Late Namurian-Westphalian, Jurassic, probable Coniacian-Santonian, probable Campanian and Early Eocene). Furthermore, apatites of metamorphic origin are much more abundant than in any of the Early Oligocene samples, indicating a fresh source of detritus.

The Early/Late Oligocene boundary also coincides with a change in depositional environment and sediment grade. Below the boundary, sediments are relatively sand-rich and were deposited in shallow marine shelf and marginal marine environments. By contrast, the overlying Late Oligocene succession is relatively sand-poor and was deposited in a deeper marine shelf environment. The major change in provenance, coupled with the major decrease in contemporaneous magmatism and the increased water depth, across the hiatus between the Early Oligocene and Late Oligocene, suggests the JA reflector records the breakup between East Greenland and the JMMC and the establishment of the proto-Kolbeinsey Ridge. This timing is consistent with the tectonostratigraphic framework proposed by Blischke et al. [15] wherein the proto-Kolbeinsey Ridge is established during Stage 4 (Oligocene).

Direct sourcing from East Greenland is one possible origin of the Late Oligocene detritus, since all the stratigraphic units represented by the reworked palynoflora outcrop

in this region. Given the evidence for separation of the JMMC from East Greenland across the Early/Late Oligocene boundary, the only feasible way to derive sediment from East Greenland during the Late Oligocene is through ice-rafting. Recent studies on sediments at Ocean Drilling Program (ODP) Site 913 in the Norwegian Sea to the northeast of Jan Mayen [53,54] have shown that ice-rafting commenced in the NE Atlantic as early as the Middle Eocene, with East Greenland being the source of the ice-rafted detritus. This is therefore one possible mechanism for sourcing of the relatively minor amounts of sand to the Jan Mayen Ridge in the Late Oligocene. The zircon ages in Oligocene sandstones near to Jan Mayen [46] are consistent with sourcing from East Greenland, with the large peak at ca. 1800–2000 Ma suggesting major input from Dronning Louise Land to the northwest by comparison with the moraine/outwash evidence [44].

However, seafloor sampling using gravity coring and dredging operations have yielded evidence for the presence of a Paleozoic-Mesozoic (Permo-Triassic, Jurassic and Cretaceous) succession in the southern Jan Mayen Ridge, a little distance south of the DSDP sites [6]. The possibility therefore exists for local sourcing, as suggested by Blischke et al. [1], although there is currently no evidence for the presence of a Carboniferous succession on the JMMC.

5.3. Middle Miocene

The Middle Miocene succession, which was found only at Site 346, includes sandstones with similar characteristics to those of the Late Oligocene. However, there is also evidence for renewed magmatic activity, manifested by a major influx of the Ti-rich amphibole kaersutite in conjunction with an increase in clinopyroxene with alkaline affinities. $^{40}\text{Ar}/^{39}\text{Ar}$ dating suggests the presence of two generations of kaersutite, one contemporaneous with sedimentation (Middle-Late Miocene, 10.3 ± 0.8 Ma) and one somewhat older (Early Miocene, 22.4 ± 0.2 Ma). The location of the igneous centre that supplied this material is uncertain, but given the proximity of Jan Mayen, which is a volcanically active island characterised by mafic alkaline rocks [55], it is tempting to suggest that the detritus represents the products of a proto-Jan Mayen volcano. Although kaersutite is not known from modern Jan Mayen lavas, it is a product of the Vesteris Seamount (Figure 1), an intraplate alkaline igneous centre that presently lies some 280 km north of Jan Mayen [56], and it is possible that the proto-Jan Mayen volcano could also have supplied kaersutite. An alternative source for the kaersutite and clinopyroxene in the Middle Miocene of the Jan Mayen Ridge might be the alkali basalts of the Vindtop Formation (dated as 13–14 Ma) that overlie the main Blosseville Group basalt pile [57]. However, there is no published petrographic information to indicate if kaersutite is associated with the Vindtop Formation.

5.4. Pleistocene

The two Pleistocene sands from the Jan Mayen Ridge have strongly contrasting mineralogies. The sample from Site 349 has a heavy mineral assemblage that consists almost exclusively of clinopyroxene, and was evidently derived from a mafic igneous source. The clinopyroxenes in this sample are predominantly subalkaline (although alkaline types are also present), and it therefore seems unlikely that they were sourced from the Jan Mayen volcano or other alkaline intraplate volcanics in the area. Since the Pleistocene succession is of glaciomarine origin [15], the source area for the clinopyroxenes could have lain some distance away: the Paleogene Blosseville Group basalts (Figure 2) appear to be their most likely source. The sample from Site 346 has a heavy mineral assemblage of predominantly metamorphic origin (epidote, garnet, calcic amphibole), similar to assemblages found in the underlying succession at both sites 346 and 349 (Figure 14). Derivation from a different part of the Greenland landmass is the most likely origin for the Pleistocene at this site. This is again compatible with the glaciomarine origin of the Pleistocene at Site 346.

6. Conclusions

Palynological and heavy mineral provenance studies have revealed a significant boundary between the Early and Late Oligocene successions on the Jan Mayen Ridge. Across this boundary, there is a marked increase in the numbers of reworked palynomorphs (including species from the Carboniferous, Jurassic, Cretaceous and Eocene), coincident with a major change in heavy mineral provenance. Below the boundary, sites 346 and 349 have strongly contrasting mineralogies indicating supply from different source rocks (both metamorphic and contemporaneous magmatic rocks). Above the boundary, the two sites have similar mineralogies, implying that the same sediment transport system supplied both sites. The boundary is also marked by a change in depositional setting, with an increase in water depth and a decrease in the abundance of sand beds. The combination of provenance change, decreased magmatism and increased subsidence suggests that the hiatus between the Early Oligocene and Late Oligocene (and hence, the JA reflector identified by Talwani et al. [15]) represents the establishment of the proto-Kolbeinsey Ridge between East Greenland and the JMMC.

During the Middle Eocene to Early Oligocene, the depositional systems appear to be relatively small in scale, as indicated by the contrasts in mineralogy between Sites 346 (and the adjacent Site 347) and Site 349 on the Jan Mayen Ridge, and between the Jan Mayen Ridge and Kap Brewster in East Greenland. The differences are manifested both in terms of igneous provenance components (Kap Brewster having a stronger subalkaline igneous signature than Site 349) and contributions from crystalline basement (Site 346 having received almost exclusively metasedimentary detritus, unlike Site 349). By contrast, in the post-Early Oligocene succession, the two sites on the Jan Mayen Ridge have similar provenance characteristics to one another.

The Jan Mayen Ridge sites provide a record of magmatism during break-up between Jan Mayen and East Greenland. At Site 349, the Middle Eocene and lower part of the Early Oligocene succession contains common indicators of input from evolved alkaline magmatic rocks, such as syenites. Higher in the succession, these become less common, with mafic magmatic sources becoming more important. Initially, both subalkaline and alkaline mafic sources are common, but the influence of alkaline mafic rocks increased with time. There is also evidence for more prolonged magmatic fractionation towards the top of the Early Oligocene. The only evidence for contemporaneous magmatic activity at Sites 346 and 347, which were influenced by a different transport system, is given by the presence of prismatic alkaline apatites, evidently of air-fall origin. The pattern seen in the Jan Mayen succession suggests that degrees of partial melting were initially low, leading to generation of alkaline (syenitic) magmas. The extent of partial melting increased during the Early Oligocene, generating basaltic rocks with both subalkaline and alkaline compositions. Towards the end of the Early Oligocene, the presence of evolved clinopyroxenes with alkaline characteristics suggest the amount of partial melting and magma supply rates both decreased. In the Late Oligocene, there is no evidence for contemporaneous igneous activity, since all the magmatic indicator minerals become less abundant. The pattern of magmatic activity reflected in the heavy mineral suite is consistent with the model of Scott et al. [10] for the formation of the JMMC, in which prolonged igneous activity during the Middle Eocene to Early Oligocene, with ejecta supplied by subaerial volcanic edifices, reflects the gradual northwards unzipping of Jan Mayen from East Greenland.

There is evidence for resumed alkaline magmatism in the vicinity of Site 346 during the Middle Miocene, marked by the presence of clinopyroxene of alkaline character and kaersutite dated as 10.3 ± 0.8 Ma and 22.4 ± 0.2 Ma. The resurgence of magmatism in the Middle Miocene either reflects intraplate alkaline activity (as presently manifested by the Jan Mayen volcano and the Vesteris Seamount), or late stage activity onshore East Greenland (as recorded by the Vindtop Formation).

Most of the magmatic indicators in the Kap Brewster succession can be ascribed to derivation from the underlying Eocene plateau basalt pile. However, there are also some

indicators for contemporaneous magmatism in the Middle Eocene, notably the presence of alkaline indicator minerals at the top of the Bopladsdalen Formation.

One problem with interpreting the Early Oligocene/Late Oligocene hiatus as a break up unconformity is the sudden influx of reworked Carboniferous-Eocene palynomorphs in the Late Oligocene succession. Thermal subsidence following the separation of Jan Mayen from East Greenland makes it unlikely that suitable lithologies were available for reworking locally, although seafloor sampling has shown the existence of a Paleozoic-Mesozoic succession on the JMMC [6]. East Greenland is a potential source of such a wide-ranging palynomorph assemblage, but by then it was separated from Jan Mayen by oceanic crust. The most likely explanation for Greenland sourcing after seafloor spreading commenced is ice-rafting, a mechanism proven to have started operating in the Norwegian Sea during the Middle Eocene [54]. Sediment sourcing by ice rafting provides a mechanism for the continued sourcing of sediment with Greenland characteristics and would also explain the increased homogeneity of sediment provenance characteristics in the Late Oligocene succession on Jan Mayen.

Supplementary Materials: The following supporting information can be downloaded at: <https://www.mdpi.com/article/10.3390/geosciences12090326/s1>.

Author Contributions: Conceptualization, A.G.W., D.P.S., D.W.J. and A.M.; methodology, D.W.J., A.M., C.M.F. and S.R.H.; formal analysis, D.W.J., A.M., C.M.F. and S.R.H.; writing—original draft preparation, A.M., D.W.J. and A.G.S.; writing—review and editing, A.M., D.W.J., A.G.S., D.P.S., C.M.F. and S.R.H. All authors have read and agreed to the published version of the manuscript.

Funding: This research received no external funding.

Data Availability Statement: Not applicable.

Acknowledgments: We are grateful to John Still (University of Aberdeen) and Iain Macdonald (Cardiff University) for their assistance with acquisition of mineral chemical data, and to Mick Pointon (CASP) for running the “R” code to assign apatite provenance. This research was carried out as part of CASP’s Greenland-Norway Project. Our sponsors’ financial support is gratefully acknowledged. We are grateful for the reviewers comments, which significantly improved the manuscript.

Conflicts of Interest: The authors declare no conflict of interest.

References

- Blischke, A.; Gaina, C.; Hopper, J.R.; Péron-Pinvidic, G.; Brandsdóttir, B.; Guarnieri, P.; Erlendsson, Ö.; Gunnarsson, K. The Jan Mayen microcontinent: An update of its architecture, structural development and role during the transition from the Ægir Ridge to the mid-oceanic Kolbeinsey Ridge. In *The NE Atlantic Region: A Reappraisal of Crustal Structure, Tectonostratigraphy and Magmatic Evolution*; Péron-Pinvidic, G., Hopper, J.R., Stoker, M.S., Gaina, C., Doornenbal, J.C., Funck, T., Árting, U.E., Eds.; Geological Society: London, UK, 2017; Special Publications Volume 447, pp. 299–337.
- Kodaira, S.; Mjelde, R.; Gunnarsson, K.; Shiobara, H.; Shimamura, H. Structure of the Jan Mayen microcontinent and implications for its evolution. *Geophys. J. Int.* **1998**, *132*, 383–400. [[CrossRef](#)]
- Mjelde, R.; Eckhoff, I.; Solbakken, S.; Kodaira, S.; Shimamura, H.; Gunnarsson, K.; Nakanishi, A.; Shiobara, H. Gravity and S-wave modelling across the Jan Mayen Ridge, North Atlantic; implications for crustal lithology. *Mar. Geophys. Res.* **2007**, *28*, 27–41. [[CrossRef](#)]
- Breivik, A.J.; Mjelde, R.; Faleide, J.I.; Murai, Y. The eastern Jan Mayen microcontinent volcanic margin. *Geophys. J. Int.* **2012**, *188*, 798–818. [[CrossRef](#)]
- Kandilarov, A.; Mjelde, R.; Pedersen, R.B.; Hellevang, B.; Papenberg, C.; Petersen, C.J.; Planert, L.; Flueh, E. The northern boundary of the Jan Mayen microcontinent, North Atlantic, determined from ocean bottom seismic, multichannel seismic, and gravity data. *Mar. Geophys. Res.* **2012**, *33*, 55–76. [[CrossRef](#)]
- Polteau, S.; Mazzini, A.; Hansen, C.; Planke, S.; Jerram, D.A.; Millett, J.; Abdelmalak, M.A.; Blischke, A.; Myklebust, R. The pre-breakup stratigraphy and petroleum system of the Southern Jan Mayen Ridge revealed by seafloor sampling. *Tectonophysics* **2019**, *760*, 152–164. [[CrossRef](#)]
- Brandsdóttir, B.; Hooft, E.; Mjelde, R.; Murai, Y. Origin and evolution of the Kolbeinsey Ridge and Iceland Plateau, N-Atlantic. *Geochem. Geophys. Geosystems* **2015**, *16*, 612–634. [[CrossRef](#)]
- Bott, M.H.P. The continental margin of central East Greenland in relation to North Atlantic plate tectonic evolution. *J. Geol. Soc.* **1987**, *144*, 561–568. [[CrossRef](#)]

9. Kuvaas, B.; Kodaira, S. The formation of the Jan Mayen microcontinent: The missing piece in the continental puzzle between the Møre-Vørings Basins and East Greenland. *First Break* **1997**, *15*, 239–247. [[CrossRef](#)]
10. Scott, R.A. Mesozoic–Cenozoic evolution of East Greenland: Implications of a reinterpreted continent–ocean boundary location. *Polarforschung* **2000**, *68*, 83–91.
11. Gaina, C.; Gernigon, L.; Ball, P. Palaeocene–Recent plate boundaries in the NE Atlantic and the formation of the JMMC. *J. Geol. Soc.* **2009**, *166*, 601–616. [[CrossRef](#)]
12. Gernigon, L.; Franke, D.; Geoffroy, L.; Schiffer, C.; Foulger, G.R.; Stoker, M. Crustal fragmentation, magmatism, and the diachronous opening of the Norwegian-Greenland Sea. *Earth Sci. Rev.* **2019**, *193*, 102839. [[CrossRef](#)]
13. Schiffer, C.; Peace, A.; Phethean, J.; Gerginon, L.; McCaffrey, K.; Petersen, K.D.; Foulger, G.R. The Jan Mayen microplate complex and the Wilson cycle. In *Fifty Years of the Wilson Cycle Concept in Plate Tectonics*; Wilson, R.W., Houseman, G.A., McCaffrey, K.J.W., Doré, A.G., Buiter, S.J.H., Eds.; Geological Society: London, UK, 2018; Special Publications Volume 470, pp. 393–414.
14. Blischke, A.; Stoker, M.S.; Brandsdóttir, B.; Hopper, J.R.; Péron-Pinvidic, G.; Ólavsdóttir, J.; Japsen, P. The Jan Mayen microcontinent’s Cenozoic stratigraphic succession and structural evolution within the NE-Atlantic. *Mar. Pet. Geol.* **2019**, *103*, 702–737. [[CrossRef](#)]
15. Talwani, M.; Udrinsev, G.B.; Björklund, K.; Caston, V.N.D.; Faas, R.W.; van Hinte, J.E.; Kharin, G.N.; Morris, D.A.; Mueller, C.; Nilsen, T.H.; et al. Sites 346, 347 and 349. *Initial. Rep. Deep. Sea Drill. Proj.* **1976**, *38*, 521–592.
16. Gunnarsson, K.; Sand, M.; Gudlaugsson, S.T. *Geology and Hydrocarbon Potential of the Jan Mayen Ridge*; Norwegian Petroleum Directorate: Stavanger, Norway, 1989.
17. Peron-Pinvidic, G.; Gernigon, L.; Gaina, C.; Ball, P. Insights from the Jan Mayen system in the Norwegian-Greenland Sea—I. Mapping of a microcontinent. *Geophys. J. Int.* **2012**, *191*, 385–412. [[CrossRef](#)]
18. Peron-Pinvidic, G.; Gernigon, L.; Gaina, C.; Ball, P. Insights from the Jan Mayen system in the Norwegian-Greenland Sea—II. Architecture of a microcontinent. *Geophys. J. Int.* **2012**, *191*, 413–435. [[CrossRef](#)]
19. Condon, P.J.; Jolley, D.W.; Morton, A.C. The Eocene succession on the East Shetland Platform, North Sea. *Mar. Pet. Geol.* **1992**, *9*, 633–647. [[CrossRef](#)]
20. Evans, D.; Morton, A.C.; Wilson, S.J.; Jolley, D.W.; Barreiro, B. Marine and terrestrial Tertiary sediments in BGS borehole 77/7, north of Scotland. *Scott. J. Geol.* **1997**, *33*, 31–42. [[CrossRef](#)]
21. Islam, M.A. A study of Early Eocene palaeoenvironments from the Isle of Sheppey as determined from microplankton assemblage composition. *Tert. Res.* **1984**, *6*, 11–21.
22. Costa, L.I.; Downie, C. Cenozoic dinocyst stratigraphy of Sites 403 to 406 (Rockall Plateau), IPOD, Leg 48. *Initial. Rep. Deep. Sea Drill. Proj.* **1979**, *48*, 513–529.
23. Larsen, L.M.; Pedersen, A.K.; Sørensen, E.V.; Watt, W.S.; Duncan, R.A. Stratigraphy and age of the Eocene Igertivâ Formation basalts, alkaline pebbles and sediments of the Kap Dalton Group in the graben at Kap Dalton, East Greenland. Geological Society of Denmark. *Bulletin* **2013**, *61*, 1–18. [[CrossRef](#)]
24. Storey, M.; Pedersen, A.K.; Stecher, O.; Bernstein, S.; Larsen, H.C.; Larsen, L.M.; Baker, J.A.; Duncan, R.A. Long lived postbreakup magmatism along the East Greenland margin: Evidence for shallow-mantle metasomatism by the Iceland plume. *Geology* **2004**, *32*, 173–176. [[CrossRef](#)]
25. Nielsen, T.F.D. Tertiary alkaline magmatism in East Greenland: A review. In *Alkaline Igneous Rocks*; Fitton, J.G., Upton, B.G.J., Eds.; Geological Society: London, UK, 1987; Special Publications Volume 30, pp. 489–515.
26. Upton, B.G.J.; Emeleus, C.H.; Beckinsale, R.D.; Macintyre, R.M. Myggbukta and Kap Broer Ruys: The most northerly of the East Greenland Tertiary igneous centres (?). *Mineral. Mag.* **1984**, *48*, 323–343. [[CrossRef](#)]
27. Birkenmajer, K. Report on investigations of Tertiary sediments at Kap Brewster, Scoresby Sund, East Greenland. *Rapp. Grönland Geol. Undersøgelse* **1972**, *48*, 85–91. [[CrossRef](#)]
28. Soper, N.J.; Costa, L.I. Palynological evidence for the age of Tertiary basalts and post-basaltic sediments at Kap Dalton, central East Greenland. *Rapp. Grönland Geol. Undersøgelse* **1976**, *80*, 123–127. [[CrossRef](#)]
29. Birkenmajer, K.; Jednorowska, A. Foraminiferal evidence for the East Greenland current during the Oligocene. *Rapp. Grönland Geol. Undersøgelse* **1977**, *85*, 86–89. [[CrossRef](#)]
30. Birkenmajer, K.; Jednorowska, A. Early Oligocene foraminifera from Kap Brewster, East Greenland. *Ann. Soc. Geol. Pol.* **1997**, *67*, 155–173.
31. Soper, N.J.; Downie, C.; Higgins, A.C.; Costa, L.I. Biostratigraphic ages of Tertiary basalts on the East Greenland continental margin and their relationship to plate separation in the northeast Atlantic. *Earth Planet. Sci. Lett.* **1976**, *32*, 149–157. [[CrossRef](#)]
32. Wilson, S.J. High Resolution Comparative Palynostratigraphy and Palaeoecology of Oligocene Sequences in the Terrestrial Basins of the Western British Isles and the Marine North Sea Basin. Ph.D. Thesis, University of Sheffield, Sheffield, UK, 1996.
33. Harland, R. Distribution maps of Recent dinoflagellate cysts in the bottom sediments from the North Atlantic Ocean and adjacent seas. *Palaeontology* **1983**, *26*, 321–387.
34. Eaton, G.L. Dinoflagellate cysts from the Bracklesham Beds (Eocene) of the Isle of Wight, southern England. *Bull. Br. Mus. Nat. Hist.* **1976**, *26*, 332.
35. Haq, B.U.; Hardenbol, J.; Vail, P.R. Chronology of fluctuating sea levels since the Triassic. *Science* **1987**, *235*, 1156–1167. [[CrossRef](#)]
36. Stoker, M.S.; Kimbell, G.S.; McInroy, D.B.; Morton, A.C. Eocene post-rift tectonostratigraphy of the Rockall Plateau, Atlantic margin of NW Britain: Linking early spreading tectonics and passive margin response. *Mar. Pet. Geol.* **2012**, *30*, 98–125.

37. Garzanti, E.; Padoan, M.; Andó, S.; Resentini, A.; Vezzoli, G.; Lustrino, M. Weathering and relative durability of detrital minerals in equatorial climate: Sand petrology and geochemistry in the East African Rift. *J. Geol.* **2013**, *121*, 547–580.
38. Morton, A.; Frei, D.; Stoker, M.; Ellis, D. Detrital zircon age constraints on basement history on the margins of the northern Rockall Basin. In *Exploration and Exploitation West of Shetlands*; Cannon, S., Ellis, D., Eds.; Geological Society of London: London, UK, 2014; Special Publications Volume 397, pp. 209–223.
39. Quintão, D.A.; Caxito, F.A.; Karfunkel, J.; Vieira, F.R.; Seer, H.J.; de Moraes, L.C.; Ribeiro, L.C.B.; Pedrosa-Soares, A.C. Geochemistry and sedimentary provenance of the Upper Cretaceous Uberaba Formation (Southeastern Triângulo Mineiro, MG, Brazil). *Braz. J. Geol.* **2017**, *47*, 159–182.
40. Morimoto, N.; Fabries, J.; Ferguson, A.K.; Ginzburg, I.V.; Ross, M.; Seifert, F.A.; Zussman, J.; Aoki, K.; Gottardi, G. Nomenclature of pyroxenes. *Am. Mineral.* **1988**, *73*, 1123–1133.
41. LeBas, M.J. The role of aluminium in igneous clinopyroxenes with relation to their parentage. *Am. J. Sci.* **1962**, *260*, 267–288. [CrossRef]
42. Morton, A.; Hallsworth, C.; Chalton, B. Garnet compositions in Scottish and Norwegian basement terrains: A framework for interpretation of North Sea sandstone provenance. *Mar. Pet. Geol.* **2004**, *21*, 393–410.
43. O’Sullivan, G.; Chew, D.; Morton, A.; Mark, C.; Henrichs, I. Integrated apatite geochronology and geochemistry in sedimentary provenance analysis. *Geochem. Geophys. Geosystems* **2018**, *19*, 1309–1326.
44. Morton, A.C.; Yaxley, G. Detrital apatite geochemistry and its application in provenance studies. In *Sediment Provenance and Petrogenesis: Perspectives from Petrography and Geochemistry*; Arribas, J., Critelli, S., Johnsson, M.J., Eds.; Geological Society of America: Boulder, CO, USA, 2007.
45. O’Sullivan, G.; Chew, D.; Kenny, G.; Henrichs, I.; Mulligan, D. The trace element composition of apatite and its application to detrital provenance studies. *Earth Sci. Rev.* **2020**, *201*, 103044.
46. Slama, J.; Walderhaug, O.; Fonneland, H.; Kosler, J.; Pedersen, R.B. Provenance of Neoproterozoic to upper Cretaceous sedimentary rocks, eastern Greenland: Implications for recognizing the sources of sediments in the Norwegian Sea. *Sediment. Geol.* **2011**, *238*, 254–267.
47. Szulc, A.G.; Morton, A.C.; Whitham, A.G.; Hemming, S.R.; Thomson, S.N. Establishing a provenance framework for sandstones in the Greenland–Norway rift from the composition of moraine/outwash sediments. *Geosciences* **2022**, *12*, 73. [CrossRef]
48. Gilotti, J.; Jones, K.A.; Elvevold, S. Caledonian metamorphic patterns in Greenland. In *The Greenland Caledonides: Evolution of the Northeast Margin of Laurentia*; Higgins, A.K., Gilotti, J.A., Smith, M.P., Eds.; Geological Society of America: Boulder, CO, USA, 2008; Special Paper Memoir Volume 208, pp. 201–225.
49. Nielsen, M.L.; Lee, M.; Ng, H.C.; Rushton, J.C.; Hendry, K.R.; Kihm, J.-H.; Nielsen, A.T.; Park, T.-Y.S.; Vinther, J.; Wilby, P.R. Metamorphism obscures primary taphonomic pathways in the early Cambrian Sirius Passet Lagerstätte, North Greenland. *Geology* **2021**, *50*, 4–9.
50. Morton, A.C.; Whitham, A.G.; Fanning, C.M. Provenance of Late Cretaceous–Paleocene submarine fan sandstones in the Norwegian Sea: Integration of heavy mineral, mineral chemical and zircon age data. *Sediment. Geol.* **2005**, *182*, 3–28.
51. Whitham, A.G.; Price, S.P.; Koraini, A.M.; Kelly, S.R.A. Cretaceous (post-Valanginian) sedimentation and rift events in the NE Greenland (71° – 77° N). In *Petroleum Geology of Northwest Europe: Proceedings of the 5th Conference*; Fleet, A., Boldy, S.A.R., Eds.; Geological Society of London: London, UK, 1999; pp. 325–336.
52. Peate, D.W.; Baker, J.A.; Blachert-Toft, J.; Hilton, D.R.; Storey, M.; Kent, A.J.R.; Brooks, C.K.; Hansen, H.; Pedersen, A.K.; Duncan, R.A. The Prinsen of Wales Bjerge Formation Lavas, East Greenland: The transition from tholeiitic to alkalic magmatism during Palaeogene continental break-up. *J. Petrol.* **2003**, *44*, 279–304.
53. Eldrett, J.S.; Harding, I.C.; Wilson, P.A.; Butler, E.; Roberts, A.P. Continental ice in Greenland during the Eocene and Oligocene. *Nature* **2007**, *446*, 176–179. [PubMed]
54. Tripati, A.K.; Eagle, R.A.; Morton, A.; Dowdeswell, J.A.; Atkinson, K.L.; Bahé, Y.; Dawber, C.F.; Khadun, E.; Shaw, R.M.H.; Shorttle, O.; et al. Evidence for glaciation in the Northern Hemisphere back to 44 Ma from ice rafted debris in the Greenland Sea. *Earth Planet. Sci. Lett.* **2008**, *265*, 112–122.
55. Trønnes, R.G.; Planke, S.; Sundvoll, B.; Imsland, P. Recent volcanic rocks from Jan Mayen: Low-degree melt fractions of enriched northeast Atlantic mantle. *J. Geophys. Res.* **1999**, *104*, 7153–7168.
56. Haase, K.M.; Hartmann, M.; Wallrabe-Adams, H.-J. The geochemistry of ashes from Vesterisbanken Seamount, Greenland Basin: Implications for the evolution of an alkaline volcano. *J. Volcanol. Geotherm. Res.* **1996**, *70*, 1–19.
57. Storey, M.; Duncan, R.A.; Tegner, C. Timing and duration of volcanism in the North Atlantic Igneous Province: Implications for geodynamics and links to the Iceland hot spot. *Chem. Geol.* **2007**, *241*, 264–281.